Early Evidence of San material culture represented by Organic Artifacts from Border Cave, South Africa

Francesco d'Errico, Lucinda Backwell, Paola Villa, Ilaria Degano, Jeannette J. Lucejko, Marion K. Bamford, Thomas F.G. Higham, Maria Perla Colombini, Peter P. Beaumont

Supporting Information Appendix

Archaeological context

(Text, Figure S1-S4)

Results

(Text, Figures S5-S24, Table S1-S10)

Materials and Methods

(Text)

References

(Text)

Archaeological context

Border Cave is located in the Lebombo Mountains at an elevation of 365 m above sea level, near the border between South Africa and Swaziland (27°1'19"S, 31°59'24"E). An exploratory trench was dug at the entrance of the cave by Dart in 1934. The archaeological potential and the presence of human remains was realised by Horton in 1940 while digging for guano in the middle of the cave. An excavation conducted in 1941 and 1942 by a team from the University of Witwatersrand (1) identified a long Middle Stone Age (MSA) sequence, recovered an infant burial and proposed a stratigraphic attribution to the MSA of the human remains found out of context by Horton. Excavations conducted by Beaumont from 1970 to1971 revealed further MSA, Early Later Stone Age and Iron Age horizons (2). In collaboration with L.C. Todd and G.H. Miller, Beaumont excavated the site again in 1987 (3).

The site records a 4 m thick sedimentary sequence (Fig. S1) composed of eleven main alternating brown sand (BS) and white ash (WA) deposits (4). The extreme dryness of the cavity (5) has favoured the preservation of organic material. According to Beaumont (6) and Grün and Beaumont (7) the sequence features from the bottom to the top MSA 1, Howiesons Poort, MSA 3 (= post-Howiesons Poort), and Early Later Stone Age (ELSA) lithic assemblages. The ELSA layers are overlain by a thick, virtually sterile deposit, capped by an Iron Age layer.

The post-Howiesons Poort (post-HP) is subdivided into four layers called from the bottom up 2WA, 2BS Lower C, 2BS Lower A-B, 2BS UP); the ELSA deposits are represented by three layers, 1WA at the bottom, followed by 1BS Lower C and 1BS Lower B (Fig. S1 and (8)). Above the ELSA deposits layer 1BS Lower A is an archaeologically poor, thick layer separating the ELSA from the uppermost layer 1BS UP, attributed to the Iron Age. The names of the upper layers of the sequence have changed since Beaumont's first excavations with consequences for the contextual attribution of archaeological remains, including those analysed in this paper. In the excavations conducted in the 1970s, Beaumont identified above layer 1WA three layers that he called from bottom to top 1BS Lower, 1BS UP and 1BS UP Iron Age. In the 1987 excavations the former 1BS UP was renamed 1BS Lower A. In squares V and W, where lenses were recognised in the stratigraphy, the former 1BS Lower was subdivided into sub-layers B and C (8). Organic artifacts labelled 1BS Lower come from

1970's excavations, prior to the identification of sublevels B and C in layer 1BS Lower, which does not allow their attribution to a sublevel. For this reason we refer to them as 1BS Lower B-C.

The Border Cave sequence has been dated by electron spin resonance (ESR) (5, 7, 9), amino acid racemisation (10, 11), and radiocarbon methods (12, 13, 14), which have produced ages in broad agreement. ESR results indicate that the MSA 1 layers (5WA, 5BS, 4WA, 4BS) span 227 ka to 76 ka, the Howiesons Poort layers (1 RGBS, 3WA, 3BS) range between 76 ka and 60 ka and the MSA (post-HP) layers (2WA, 2BS Lower C, 2BS Lower B and A, 2BS UP) fall between 60 ka and 37 ka BP. Forty radiocarbon ages are available for post-HP, ELSA and more recent layers, including five new ages for the ELSA layers obtained in the framework of this study and (8). Although the nine radiocarbon ages for the lower post-HP layers 2WA, 2BS Lower C and 2BS Lower B (58 to 48 ka C14 BP) fall outside the range of the IntCal09 calibration curve, which makes it problematic to interpret them in terms of calendar years, they appear in broad agreement with the range proposed by ESR for these layers.

Layer 2WA is dated to 60 ka BP, layer 2BS Lower A-B is dated to >49 ka BP. Bayesian modelling of calibrated radiocarbon ages (Fig. S2-S4) from the 2BS UP, ELSA and more recent layers (see *SI Materials and Methods*) indicate that layer 2BS Lower A is older than 49 ka BP. Layer 2BS UP accumulated between 49 ka and 45 ka BP, 1WA between 44 ka and 43 ka BP, 1BS Lower C and B between 43 ka and 42 ka BP, and 1BS Lower A between 41 ka and 22 ka BP.

With the exception of a single ^{14}C result, the ages obtained from the direct dating of organic artifacts in this study and (8) are in full agreement with those from previous studies, thus confirming the stratigraphic provenance of the artifacts. The age obtained for the poison applicator (20,420±90 OxA 23173) is in contradiction with all the dates on charcoal for sub-layers 1BS Lower B-C and the newly obtained dates on organic artifacts from the same sub-layers. It is likely that this object is intrusive from overlying 1BS Lower A, which has produced a similar ^{14}C determination (20,700±250 Pta-4984).

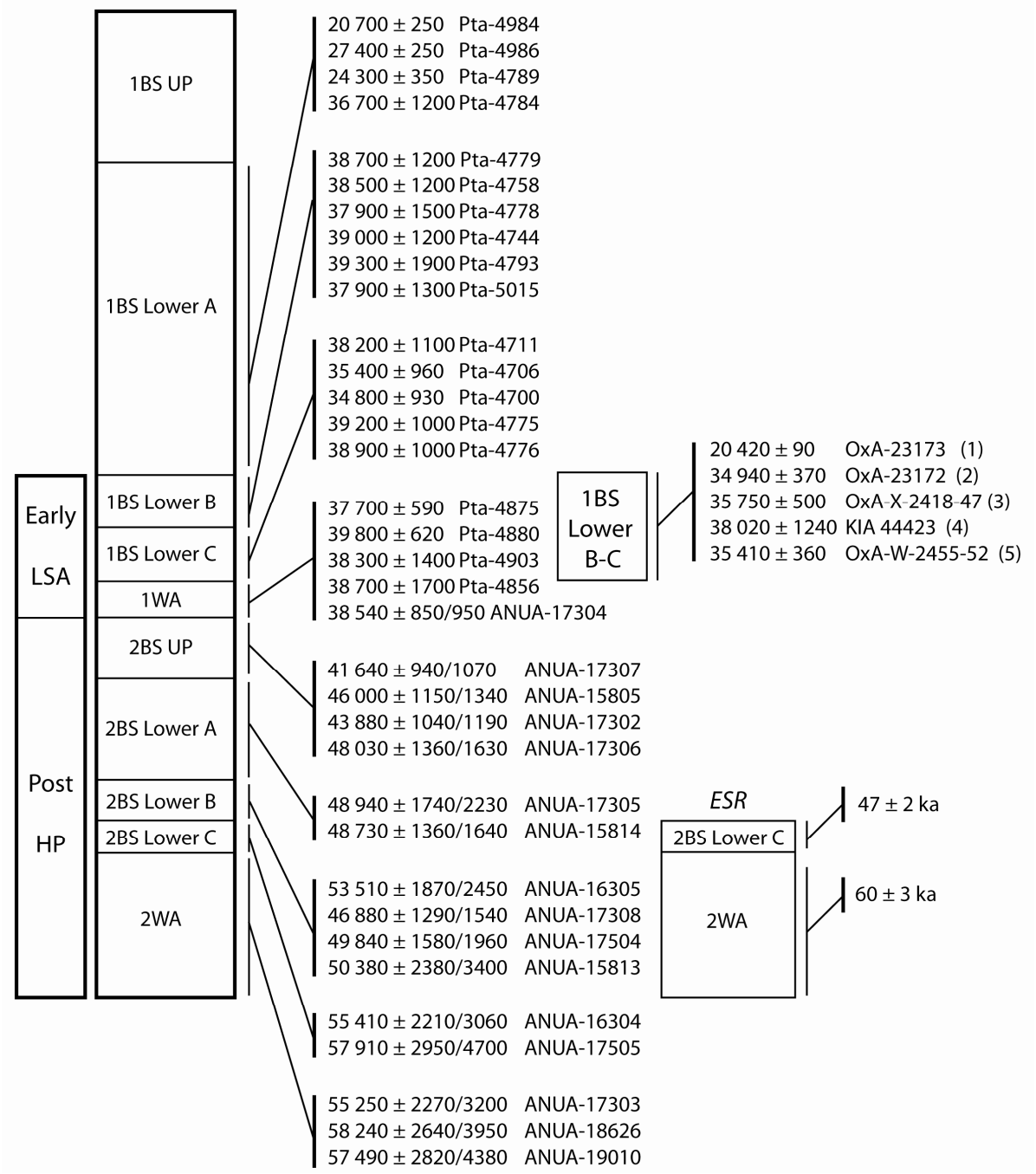

SI Figure 1. Schematic representation of the upper layers of Border Cave stratigraphy with ^{14}C and mean ESR ages. (1-5): directly dated artifacts, 1: poison applicator, 2: digging stick, 3: resin on a microlith, 4: OES bead, 5: beeswax. Radiocarbon ages after (3) and (13) with the exception of 1-5. (1, 2, 4 and 5 this study, 3: (8)); ESR ages after (3); information on the stratigraphy after (3, 5, 8, 13). Note that the ^{14}C determination ANUA-17305 is given the erroneous lab code ANUA-17304 in (13).

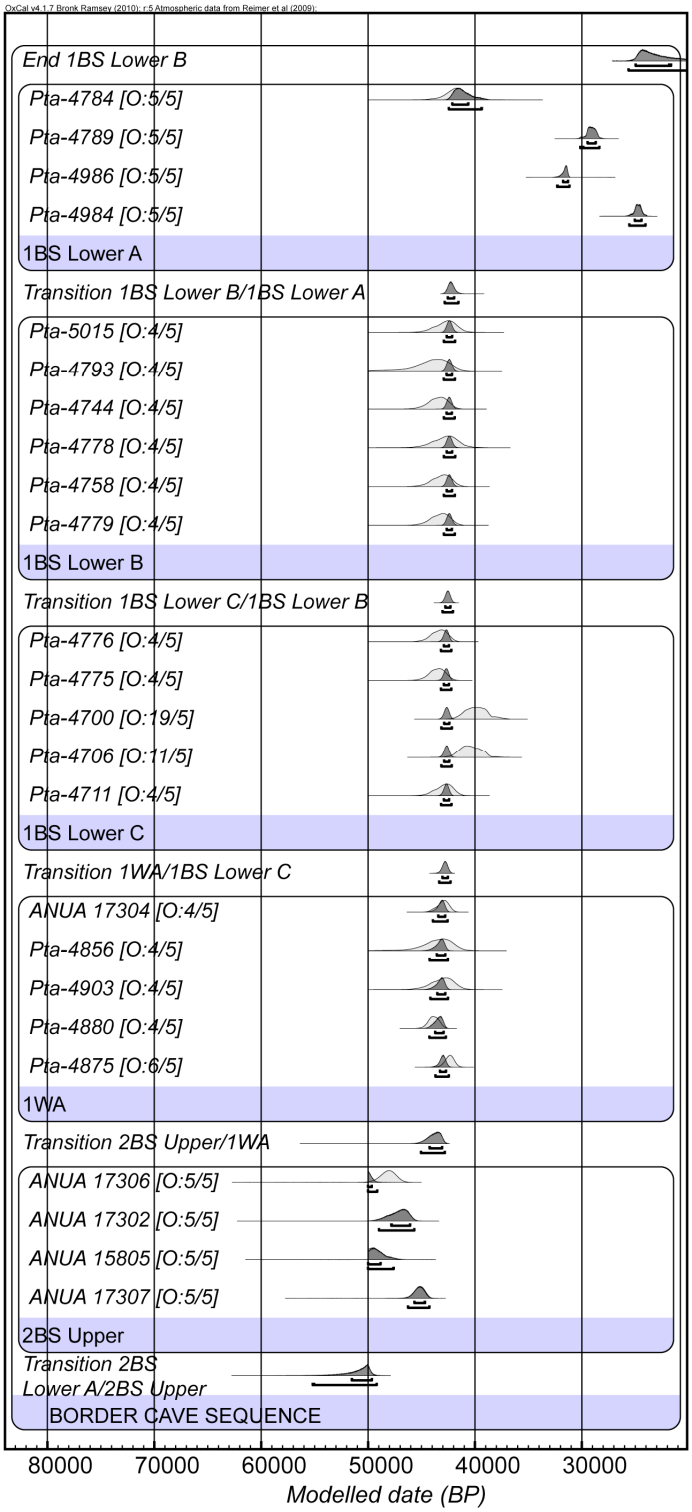

SI Figure 2. Bayesian model of radiocarbon ages from the Border Cave upper layers performed using OxCal 4.1 (14; see *SI Materials and Methods*). Figures in brackets next to the laboratory numbers denote outlier probabilities (posterior: prior).

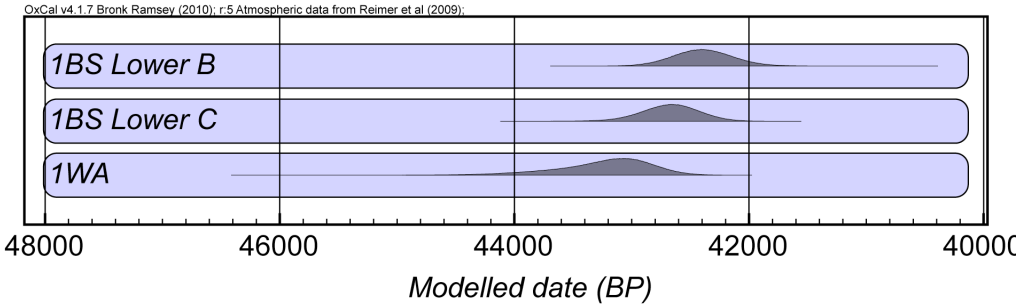

SI Figure 3. Summed probability distributions for the ranges for 1WA and 1BS lower B and C archaeological levels at Border Cave.

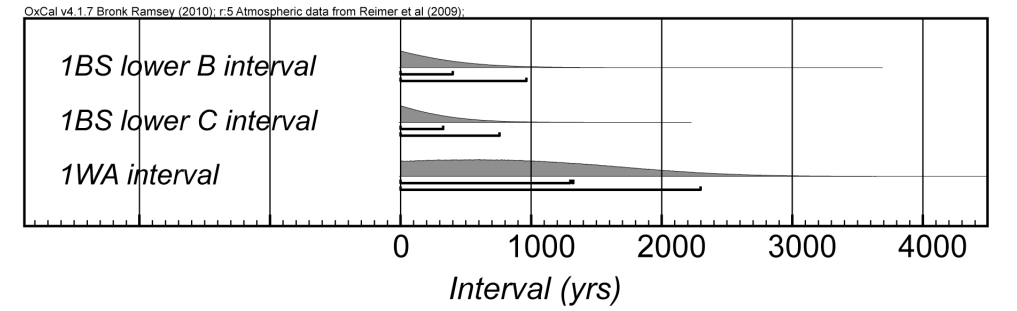

SI Figure 4. Probability distributions representing the span of time over which layers 1WA and 1BS lower B and C were occupied.

Results

Description of woods

Digging stick (layer 1BS Lower B-C; square S20). The piece of wood has no bark, is long and straight with a diameter of 13.02 mm, and a length of 175.12 mm. One end is broken but the other tip appears to be polished and rounded. The polish is an exudate of wood resin that has seeped out of the cells and hardened, appearing as an added varnish (Fig. S19a). The wood is very fine-grained and has numerous small vessels arranged in short radial multiples, very little parenchyma, tall heterocellular rays and resin. There are on average 45 vessels per mm^2 and the mean vessel tangential diameter is 27 µm (range 25-35 µm), arranged in short radial multiples of 2-5 cells, but also solitary, and some clusters occur (Fig. S19b, c). Resin occurs in some vessels and between cells (Fig. S19b). Axial

parenchyma is rare and diffuse (Fig. S19d). Medium thick walled fibres comprise the ground tissue. The fibre walls appear to have become detached from the middle lamella in some parts of the section (Fig. S19c/d). Rays are over 1 mm high and heterocellular with alternating broad bands of procumbent body cells and 8 or more upright cells (Fig. S19e). In transverse section the rays are 1 – 3 cells wide (Fig. S19b/d). In longitudinal section shiny crystals can be seen in the procumbent and upright ray cells, but it is not possible to see their shape or number (Fig. S19e), nor the perforation plates or intervessel pitting. The wood has been compared with *Dovyalis caffra, Dovyalis ziziphoides, Scolopia mundii, Scolopia zeyheri* (Salicaceae (Flacourtiaceae), *Catha edulis* (Celastraceae) and *Heywoodia lucens* (Phyllanthaceae (Euphorbiaceae) as some wood anatomy features overlap.

Poison applicator (layer 1BS Lower B-C; square Q21). The pieces have no bark and are covered with shallow, straight incisions. The analysed piece is 4.72 mm in diameter and 82.94 mm long, with the same general wood anatomical features as the digging stick, but some of the measurements differ. There are 80 vessels per mm^2 yet this number may be inflated by the inclusion of parenchyma cells that are nearly as big as the vessels (Fig. S19f). The vessel mean tangential diameter is 25 µm (range 20 – 35 µm). The rays are over 1.5 mm high.

Identification

Not all the useful features for identification are visible, so several possible options are given here. The most distinctive feature of the wood is the very high heterocellular rays comprising alternating bands of procumbent body cells and more than eight rows of square cells, as seen in radial longitudinal section. Both types of ray cells contain crystals. The parenchyma is rare and diffuse. Vessels are small, numerous and in radial multiples. Individually these features are common but their combination is rare.

From the keys used there are seven comparable taxa and these are discussed below. Two species of *Dovyalis, D. caffra* and *D. ziziphoides* of the Salicaceae (Flacourtiaceae in older literature; 15) are similar to the Border Cave specimens, but based on the wood anatomy alone the living species are indistinguishable. The two species are characterised by numerous small diameter vessels in short radial multiples, minute to small alternate intervessel pits, thin to thick-walled fibres, absent to rare axial parenchyma, and rays that are more than 1 mm high, 1-3 cells wide and heterocellular with

procumbent body cells with more than four rows of square marginal cells. Prismatic crystals occur in the procumbent and square ray cells. The widths of the uniseriate and multiseriate portions of the rays are equal. In the archaeological specimens from Border Cave it is not possible to see the intervessel pitting. The archaeological specimens have deposits of gum or resin in some of the vessels, and even between cells, but this feature is not mentioned in the modern woods. The Border Cave wood differs from the modern *Dovyalis* species in the arrangement of the ray cells.

Scolopia mundii and *Scolopia zeyheri*, also members of the Salicaceae, are similar to the Border Cave woods, but both have wider rays. However, *S. mundii* has gum or resin in the vessels. *Catha edulis* (Celastraceae) is similar, but its distinguishing feature is the alternating bands of parenchyma-like fibres and ordinary fibres. This feature is not recognisable in the very small archaeological specimens. Two taxa from the Euphorbiaceae are closely comparable. *Flueggea virosa* (previously *Securinega virosa;* 16, 17*)* has radial multiples of vessels and gum in the ray cells and crystals. *Heywoodia lucens* (Phyllanthaceae (Euphorbiaceae)) also has long radial multiples, rare diffuse parenchyma, and rays with 3-seriate body sections of procumbent cells, and long tails of 4-10 square to upright cells, the latter containing rare prismatic crystals. The rays of both woods of the Euphorbiaceae can overlap and appear to have alternating bands of procumbent and upright cells. The key difference between the two species is the presence of scalariform perforation plates in *Heywoodia lucens* and simple perforation plates in *Flueggea virosa* (17). The thin sections of the archaeological samples show only simple perforation plates, so the wood is identified as *Flueggea virosa*. This wood most closely resembles the archaeological specimens.

Habitat, distribution and uses

Border Cave is in the moist savanna biome near the Lebombo Mountains, which have low altitude bushveld and forest on the top. All of the seven taxa discussed here could occur in the region. The trees or shrubs known to have useful wood are *Scolopia mundii, S. zeyheri, Catha edulis, Securinega virosa* and *Heywoodia lucens* (16, 18). Of these seven, only *Flueggea (Securinega*) *virosa* has been recorded as being used for arrow shafts and many other implements throughout southern, western and eastern Africa (18).

Chemical analysis of the wood comprising the poison applicator

The results obtained with pyrolysis are reported in Fig. S20, which shows the total ion chromatograms of samples of archaeological wood material, specifically samples collected from the poison applicator and the digging stick (samples 46c and 47a respectively). Table S6 lists the products obtained from pyrolysis of these samples in the presence of hexamethyldisilazane (HMDS). The pyrograms are mainly characterized by pyrolysis products originating from cellulose (C, carbohydrates), while only two peaks (#16, #53) are due to the presence of lignin (G, guaiacyl units). The low content of lignin and the high content of polysaccharides indicate that the samples were probably cut from a bush-type plant. The presence of only guaiacyl (methoxyphenols) lignin units and the absence of syringyl (dimethoxyphenols) units in the pyrolysis profile may suggest that both the analysed samples belong to gymnosperms (softwood). The low abundance of lignin units in general, and the high degradation of the samples do not allow for an ultimate identification in the absence of relevant reference materials. The comparison with *Securinega virosa* or *Heywoodia lucens* (*Euphorbiaceae*) did not show satisfactory matches in the pyrolysis profile.

Chemical analysis of the residue on the poison applicator

Two samples were collected from the tip and the central part of the poison applicator (samples 46a and 46cr respectively) and were analysed for the detection of both sugars and lipid-resinous materials. Neither sample contained sugars above the detection limit of the procedure. Both samples contained resinous and lipid materials; the chromatogram of sample 46a is shown in Fig. 2 (n. 27), while the list of peaks detected is given in Table S7. Linear monocarboxylic acids with even and odd number of carbon atoms, ranging from 12 to 20 atoms and showing a maximum with palmitic acid (#8) and linear α,ω-dicarboxylic acids ranging from 8 to 12 carbot atoms and showing a maximum with α,ω-nonanedienoic acid (#19) were identified. Linear hydrocarbons ranging from 24 to 31, linear alcohols with 16, 18 and 20 carbon atoms, cholesterol and sitosterol were detected. In both samples, unsaturated monocarboxylic acids (C16:1 (palmitoleic), C18:2 (linoleic), C18:1 (oleic and elaidic)) are present. Unsaturated 12-hydroxy-9-octadecenoic acids (ricinoleic and ricinelaidic) are present only in sample 46a, but not in sample 46cr. Cholesterol is most probably a contaminant. The presence of mono and dicarboxylic acids suggest the presence of a lipid material; the occurrence of both *cis* and *trans* isomers of unsaturated carboxylic acids suggest that the material was heated. In addition, the simultaneous presence of even and odd chain length hydrocarbons may suggest the

presence of cuticular wax (19). Ricinoleic acid can be found in mature castor beans (*Ricinus communis* L., *Euphorbiaceae*), but it is also present in the sclerotium of ergot (*Claviceps purpurea* Tul. or *Claviceps africana*, *Clavicipitaceae*), which grows on crops (20). Some unknown compounds were detected (peaks #25, 28, 30) whose mass spectra are consistent with hydroxy-carboxylic acids, both saturated and unsaturated.

Analysis of the lump of organic material

Two microsamples were collected from the outer, darker area of the lump and from the inner, lighter one (samples 7 and 7* respectively) and were analysed in order to determine lipids, resins, saccharides and proteic materials. Each sample was ground prior to analysis.

Polysaccharide analysis: Saccharides were detected at blank level, below the detection limit of the analytical procedure.

Protein analysis: The samples contain a relevant amount of amino acids (above quantitation limit) whose profile matches that of egg (21). The selected ion monitoring (SIM) chromatogram of amino acids in sample 7* directly submitted to hydrolysis is shown in Fig. S24. Principal component analysis (PCA) performed on a database comprising egg, casein and animal glue samples confirmed this hypothesis. The total proteic content was around 0.5% of the whole sample in both cases. It is important to note that external contamination cannot be excluded.

Resinous lipid material analysis: The chromatogram of sample 7 is shown in Fig. 2 (n.28), and the identified peaks are listed in Table S9. The chromatograms for both samples (7 and 7*) are comparable.

In sum, linear monocarboxylic acids with an even number of carbon atoms (ranging from 12 to 30 atoms and showing a maximum with palmitic acid (#11)), and linear (ω-1) hydroxy acids with an even number of carbon atoms (ranging from 16 to 24 atoms and showing a maximum with 15-hydroxy hexadecanoic acid (#18)) were identified. Linear hydrocarbons with an odd number of carbon atoms (ranging from 19 to 33 and showing a maximum with heptacosane (#27)), linear alcohols with an even number of carbons (ranging from 16 to 34 and showing a maximum with triacontanol (#42)), linear α-(ω-1) diols with an even number of carbons (1,23-tetracosanediol and 1,25-hexacosanediol) were identified. This profile is in perfect agreement with literature data on the composition of beeswax (22, 23) and thus beeswax is the main organic constituent of the samples. At high retention times triterpenes are detected, the presence of which points to the occurrence of a

natural triterpenoid resin in the sample. We identified: β-amyrin (peak # 41), lupeol, Δ^{18} friedelen-3-ol, Δ^{18} friedelen-3-one (identified on the basis of the interpretation of their mass spectra and data from the literature (24)) and unknown triterpenes (#42, coeluting with triacontanol, #47, 48 and 49). Peak 44 was identified as cycloartanol, which is a sterol precursor in photosynthetic organisms and plants. Peak 47 is characterised by the presence of m/z = 143, which suggests the presence of an ocotillone type molecule (degradation/oxidation product of the triterpenes).

A review of the literature (25) indicates that the nature and profile of the identified triterpenes may be linked to the presence of a resin extracted from *Euphorbia tirucalli*. In order to test this hypothesis, the bark and the wood of this species were extracted with organic solvents (CH_2Cl_2/MeOH 2:1) and subjected to the same procedure as the archaeological samples. In the plant extracts, β-amyrone, Δ^{18} friedelen-3-one, β-sitosterol, Δ^{18} friedelen-3-ol, lup-20(29)-2en-3-one, β-amyrin and lupeol were detected. Results show that it is very likely that the triterpenes identified in the archaeological sample are due to the presence of *Euphorbia tirucalli* resin and its oxidation products in the beeswax.

SI Table 1. Dimensions of Border Cave organic artifacts

Layer	Square	Description	Raw Material	Length	Width	Thick.	PerfMax	PerfMin
1BS Lower B-C	W16	point	bone	31.80*	3.42*	1.70	-	-
1BS Lower B-C	Q23	point	bone	51.38*	4.98	4.18	-	-
1BS Lower B-C	T18	notched object	bone (5)	76.01*	8.50	5.75	-	-
1BS Lower B-C	S19	bead	gastropod	7.78	6.73	na	2.89	2.82
1BS Lower B-C	T20	point+	bone	38.17*	3.20*	2.60	-	-
1BS Lower B-C	Q21	preform	tusk (2)	86.40*	13.70	7.30	-	-
1BS Lower B-C	R23	bead	OES	8.43	8.43	na	3.18	3.24
1BS Lower B-C	R24	bead	OES	4.46	4.15	1.39	1.72	1.66
1BS Lower B-C	R22	bead	OES	9.12	8.35	1.81	3.11	3.00
1BS Lower B-C	Q16	point	tusk (2)	62.92	11.79	4.31	-	-
1BS Lower B-C	Q21	notched stick frag.++	wood	82.94*	5.50	4.72	-	-
1BS Lower B-C	Q21	notched stick frag.	wood	98.30*	5.36	4.70	-	-
1BS Lower B-C	Q21	notched stick frag.	wood	88.25*	5.20	5.08	-	-
1BS Lower B-C	Q21	notched stick frag.	wood	53.36*	4.35	4.22	-	-
1BS Lower B-C	S20	digging stick tip	wood (4)	175.12*	15.59	13.02	-	-
1BS Lower B-C	S19	lump with vegetal	beeswax	39.56	34.63	15.02	-	-
1WA	V21	notched rib	bone	43.02*	15.50	1.98	-	-
1WA	W16	notched object	bone	12.02*	5.96*	2.34	-	-
1WA	R18	bead	gastropod	7.75	6.58	na	4.13	2.76
1WA	T22	shaped frag.	tusk (2)	28.47*	10.57	3.93	-	-
1WA	T22	awl	bone	28.63*	7.59*	4.36*	-	-
1WA	Q17	awl	bone	99*	5.19*	10.91*	-	-
1WA	S19	point frag.+	bone	23.34*	3.60*	2.49	-	-
1WA	S19	shaped frag.	bone	22.02*	5.37	3.92	-	-
1WA	Q19	bead	OES	-	-	-	-	-
1WA	Q24	bead	OES	7.67	7.52	2.15	2.97	2.88
1WA	Q24	bead	OES	6.99	6.61	na	2.77	2.77
1WA	T18	bead	OES	6.62	6.64	1.45	2.94	2.82
1WA	S23	bead	OES	7.15	6.67	1.68	2.49	2.39
1WA	S23	bead	OES	6.45	6.08	1.64	-	-
1WA	R20	bead	OES	8.31	7.28	2.17	3.01	3.01
1WA	S19	bead	OES	8.05	7.11	1.81	2.26	2.16
1WA	T19	bead	OES	6.63	6.26	1.74	3.15	2.89
1WA	T19	bead	OES	6.01	5.56	-	2.75	2.61
1WA	R19	bead	OES	8.10	7.87	-	2.92	2.72
2BS(LR.C)	S21	indet	tusk (2)	59.82*	7.56*	3.42	-	-
2BS(LR.C)	R20	indet	tusk (2)	78.90*	14.77	4.43	-	-
2BS(LR.C)	S23	awl	tusk (1)	129.89*	19.49	8.02	-	-
2WA	T19	notched object	bone	37.86*	14.91	7.52	-	-
2WA	Q21	awl	tusk (2)	89.04*	15.83	5.95	-	-
2WA	R18	shaped frag.	tusk (2)	45.38*	8.05	3.42	-	-

Thick.: thickness; Tech.: technique; PerMax: Perforation maximum diameter; PerMin: perforation minumum diameter;
1: warthog; 2: warthhog or bushpig. 3: Nassarius kraussianus; 4: identification? ; 5: baboon fibula
OES: ostrich egg shell; S: scraped; I: incised; G: ground; B: bound; P: perforated; E: engraved; + ochre residue;
++ resin residue; frag.: fragment

SI Table 2. Dimensions of archaeological and ethnographic bone points.

	Cultural	5 mm		10 mm		30 mm	
Site	**attribution**	**width**	**thickness**	**width**	**thickness**	**width**	**thickness**
Border Cave (1BS LR.B-C)	ELSA	1.78	1.43	2.06	1.53	2.70	1.54
Border Cave (1BS LR.B-C)	ELSA	2.01	1.97	2.70	2.65	3.82	3.52
Border Cave (1BS LR.B-C)	ELSA	1.49	1.48	1.92	1.61	2.31	2.26
BorderCave (1WA)	ELSA	1.26	0.95	1.83	1.31	3.19	2.01
Blombos Cave	MSA (Still Bay)	3.00	2.50	4.10	3.60	6.80	5.40
Blombos Cave	MSA (Still Bay)	3.20	2.50	4.80	3.20	7.70	5.80
Blombos Cave	MSA (Still Bay)	4.00	2.50	7.50	4.50	11.00	6.50
Peers	MSA (Still Bay?)	2.80	2.20	3.50	3.20	5.80	5.10
Sibudu	MSA (HP)	2.11	2.06	3.23	2.95	5.24	5.00
Klasies	MSA (HP?)	2.00	1.90	3.00	2.50	4.60	3.80
Jubilee Shelter	LSA (Wilton)	2.03	1.72	2.33	2.61	3.65	3.23
Jubilee Shelter	LSA (Wilton)	1.78	1.80	2.34	2.32	4.30	2.70
Jubilee Shelter	LSA (Wilton)	1.90	1.87	2.28	2.46	3.12	3.05
Jubilee Shelter	LSA (Wilton)	1.47	1.39	1.36	1.66	2.47	2.30
Jubilee Shelter	LSA (Wilton)	1.59	1.47	2.09	2.05	3.05	3.03
Mapungubwe K2	Iron Age	1.44	1.37	1.95	1.80	2.94	2.53
Mapungubwe K2	Iron Age	1.56	1.80	2.02	2.37	3.60	3.54
Mapungubwe K2	Iron Age	1.87	1.94	2.27	2.44	3.42	3.31
Mapungubwe K2	Iron Age	1.46	1.72	1.92	2.02	3.26	2.95
Mapungubwe K2	Iron Age	1.63	1.49	2.08	1.94	3.61	3.18
Mapungubwe K2	Iron Age	1.54	1.53	2.08	2.12	3.83	3.60
Mapungubwe K2	Iron Age	1.51	1.56	2.09	2.20	3.64	3.46
Mapungubwe K2	Iron Age	1.67	1.86	2.32	2.45	3.68	3.54
Mapungubwe K2	Iron Age	1.68	1.58	2.17	2.13	3.59	3.55
Mapungubwe K2	Iron Age	1.42	1.51	1.81	1.80	3.07	3.04
Mapungubwe K2	Iron Age	1.67	1.64	2.30	2.44	3.76	3.66
Mapungubwe K2	Iron Age	1.55	1.46	1.93	1.92	3.23	3.21
Mapungubwe K2	Iron Age	1.62	1.59	2.07	2.11	3.14	3.11
Mapungubwe K2	Iron Age	1.56	1.60	2.11	2.01	3.31	3.26
Mapungubwe K2	Iron Age	1.79	1.72	2.40	2.36	3.72	3.61
Mapungubwe K2	Iron Age	1.64	1.60	2.06	1.91	2.67	2.58
Mapungubwe K2	Iron Age	1.61	1.84	2.24	2.00	3.40	3.37
Mapungubwe K2	Iron Age	1.74	1.77	2.31	1.93	3.62	3.32
Mapungubwe K2	Iron Age	1.83	1.94	2.43	2.28	3.78	3.40
Mapungubwe K2	Iron Age	1.54	1.59	2.04	1.99	3.09	3.07
Mapungubwe K2	Iron Age	1.86	1.88	2.21	2.29	3.54	3.08
Mapungubwe K2	Iron Age	2.18	2.25	2.75	2.76	4.18	3.93
Mapungubwe K2	Iron Age	1.83	1.69	2.19	2.11	2.96	2.93
Mapungubwe K2	Iron Age	1.90	1.99	2.49	2.69	3.91	3.78
Mapungubwe K2	Iron Age	2.17	2.28	2.66	2.62	3.54	3.40

San (Fourie Collection)	San	2.23	2.10	2.64	2.43	3.33	3.06
San (Fourie Collection)	San	2.08	1.97	2.89	3.08	4.50	4.50
San (Fourie Collection)	San	1.78	1.70	2.46	2.23	3.54	3.27
San (Fourie Collection)	San	1.88	1.71	2.11	2.22	3.34	3.17
San (Fourie Collection)	San	2.10	2.03	2.79	2.99	4.27	4.11
San (Fourie Collection)	San	2.96	2.87	3.98	3.92	5.97	5.91
San (Fourie Collection)	San	1.70	1.61	2.21	2.14	3.38	3.52
San (Fourie Collection)	San	1.78	1.75	2.33	2.20	3.67	3.37
San (Fourie Collection)	San	1.91	1.86	2.87	2.78	4.00	3.62
San (Fourie Collection)	San	1.80	1.79	2.21	2.22	3.42	3.22
San (Fourie Collection)	San	1.28	1.22	1.87	1.81	3.12	2.61
San (Fourie Collection)	San	1.96	1.94	2.55	2.57	3.77	3.56
San (Fourie Collection)	San	1.43	1.33	1.70	1.69	3.10	2.11
San (Fourie Collection)	San	1.73	1.69	2.57	2.59	3.73	3.63
San (Fourie Collection)	San	1.83	1.81	2.39	2.21	3.27	3.16
San (Fourie Collection)	San	1.86	1.77	2.47	2.38	3.33	3.06
San (Fourie Collection)	San	2.39	2.39	3.23	3.36	4.62	4.26
San (Fourie Collection)	San	2.34	2.29	2.84	2.78	4.04	4.02
San (Fourie Collection)	San	2.02	1.70	2.46	2.48	3.51	3.50
San (Fourie Collection)	San	1.87	1.70	2.32	2.36	3.79	3.72
San (Fourie Collection)	San	1.62	1.50	2.02	2.03	3.18	3.14
San (Fourie Collection)	San	1.50	1.46	1.86	1.96	2.83	2.81
San (Fourie Collection)	San	2.17	2.04	2.67	2.76	3.93	3.66
San (Fourie Collection)	San	1.93	1.92	2.15	2.35	3.40	3.37
San (Fourie Collection)	San	2.35	2.25	2.61	2.71	3.48	3.11
San (Fourie Collection)	San	2.36	2.32	3.03	3.05	4.68	4.58
San (Fourie Collection)	San	2.98	2.82	3.29	3.43	4.51	3.76
San (Fourie Collection)	San	1.88	1.80	2.32	2.38	4.21	4.20
San (Fourie Collection)	San	1.84	1.62	2.09	2.34	3.95	3.75
San (Fourie Collection)	San	1.46	1.45	2.07	2.06	3.48	2.98
San (Fourie Collection)	San	2.45	2.37	2.57	3.08	4.08	3.93
San (Fourie Collection)	San	1.27	1.05	1.66	1.88	3.05	2.56
San (Fourie Collection)	San	1.67	1.57	1.93	2.17	3.18	3.16
San (Fourie Collection)	San	1.49	1.42	1.97	1.95	2.93	2.92
San (Fourie Collection)	San	1.79	1.66	2.26	2.37	3.62	3.51
San (Fourie Collection)	San	1.42	1.38	1.69	1.78	2.78	2.76
San (Fourie Collection)	San	1.93	1.71	2.12	1.97	3.44	3.17
San (Fourie Collection)	San	1.75	1.66	2.43	2.35	3.88	3.79
San (Fourie Collection)	San	1.99	1.92	2.99	2.62	4.10	3.84
San (Fourie Collection)	San	1.61	1.57	1.89	1.98	2.86	2.64
San (Fourie Collection)	San	2.00	1.87	2.46	2.59	3.60	3.53
San (Fourie Collection)	San	1.61	1.58	2.18	2.22	3.64	3.54
San (Fourie Collection)	San	2.42	2.29	2.86	2.91	4.01	3.90
San (Fourie Collection)	San	2.34	2.17	3.02	3.04	4.45	4.27
San (Fourie Collection)	San	1.47	1.42	1.87	1.82	2.93	2.84
San (Fourie Collection)	San	1.66	1.55	1.86	1.94	3.35	2.96
San (Fourie Collection)	San	1.80	1.66	2.19	2.15	3.02	2.98
San (Fourie Collection)	San	1.13	1.11	1.53	1.53	2.44	1.97
San (Fourie Collection)	San	1.57	1.49	1.94	2.14	3.19	3.07
San (Fourie Collection)	San	1.83	1.63	2.23	2.36	3.37	3.22

SI Table 3. Contex and description of OES beads from Border Cave ELSA layers

Layer	Square	Production Stage	Perf. shape	Burnt	Ochre	Worn	Diameter		Thick.	Aperture	
							Max.	Min.		Max	Min
1BS Lower B-C	R 23	finished	co			●	8.43	8.43	-	3.18	3.24
1BS Lower B-C	R24	finished	co			●	4.46	4.15	1.39	1.72	1.66
1BS Lower B-C (1)	R22	finished	cy			●	9.12	8.35	1.81	3.11	3.00
1WA	Q19	finished	cy			●	-	-	-	3.1	2.7
1WA	Q24	finished	cy			●	7.67	7.52	2.15	2.97	2.88
1WA	Q24	finished	cy	●		●	6.99	6.61	na	2.77	2.77
1WA	T18	finished	cy	●		●	6.62	6.64	1.45	2.94	2.82
1WA	S23	finished	co			●	7.15	6.67	1.68	2.49	2.39
1WA	S23	finished	cy			●	6.45	6.08	1.64	2.4	2.3
1WA	R20	preform*	co				8.31	7.28	2.17	3.01	3.01
1WA	S19	finished	co			●	8.05	7.11	1.81	2.26	2.16
1WA	T19	finished	cy			●	6.63	6.26	1.74	3.15	2.89
1WA	T19	finished	cy	●	●	●	6.01	5.56	-	2.75	2.61
1WA	R19	preform*	co	●	●		8.10	7.87	-	2.92	2.72

* stage 9 of manufacture according to (26), Thick.: thickness; Tech.: technique; Max: maximum; Min: minumum; G: ground; Perf: perforation; + ochre residue

(1) directly dated by AMS to 38020 +1240/-1070 BP (KIA-44423)

SI Table 4. OES beads size variability in archaeological assemblages *

Site	Layer	Cultural Attribution	Diameter (mm)					Aperture (mm)	
			n	Mean	Std. Dev.	Min	Max	Mean	Std. Dev.
Border Cave	1BS Lower B-C	ELSA	3	7.33	2.51	4,46	9.12	2.67	0.82
Border Cave	1WA	ELSA	8	6.94	0,66	6.01	8.05	2.71	0.30
Border Cave	1WA & 1BS L	ELSA	11	7,05	1.26	4.46	9.12	2.70	0.45
Geelbek Dunes	small beads	LSA	272	3.10	0.32	2.30	4,9	1.52	0.33
Geelbek Dunes	large beads	LSA	5	6,68	0.99	5.30	7.80	3.04	0.73
JKB N	-	LSA	135	4.09	0.59	2.80	6.50	1.59	0.34
JKB L	-	LSA	139	4.56	0.60	2.60	6.55	1.45	0.22
JKB M	-	LSA	20	4.88	0.96	3.60	7.05	2.12	0.43
KN2005/067	-	LSA	9	5.62	0.11	5.26	5.56	2.78	0.09
SK2005/057A	-	LSA	26	5.59	0.41	4.11	6.36	1.98	0.50
LNC	spit 1	LSA	4	5.10	1.70	3.50	7.00	-	-
LNC	spit 2	LSA	5	5.10	0.70	4.00	5.50	-	-
LNC	spit 4	LSA	17	5.20	1.10	4.00	7.00	-	-
LNC	spit 5	LSA	40	4.80	0.80	3.00	7.00	-	-
LNC	spit 6	LSA	50	4.90	0.80	3.00	7.50	-	-
LNC	spit 7	LSA	19	4.60	0.70	3.00	5.50	-	-
Zais	-	LSA	19	5.00	0.60	4.00	6.00	-	-
OLS	1	LSA	14	6.00	3.40	3.00	15.00	-	-
OLS	2	LSA	12	4.70	1.00	3.00	6.00	-	-
Geduld	-	LSA	80	5.90	1.00	4.00	8.00	-	-
Eros	-	LSA	8	6.30	1.20	5.00	9.00	-	-
Wortel	-	LSA	48	8.50	1.80	5.00	12.00	-	-
K	23	LSA	41	6.20	1.60	4.00	10.00	-	-
K	24	LSA	6	5.80	0.90	4.50	6.50	-	-
K	25	LSA	42	8.00	1.90	4.50	12.00	-	-
K	26	LSA	170	6.80	2.00	4.00	13.50	-	-
K	27	LSA	26	5.40	1.30	4.50	10.00	-	-
K	28	LSA	10	7.10	1.80	5.00	10.50	-	-
Siphiso	I-V	LSA	52	5.59	0.86	3.50	7.80	1.91	0.36
Siphiso	VI-VII	LSA	72	6.86	1.18	4.00	10.00	2.83	0.67
Siphiso	VIII-IX	LSA	15	5.78	1.49	4.10	9.00	2.17	0.88

* data from (26-29)

JKB: Jakkalsberg; LNC: Lower Numas Cave; OLS: Orabes Lower Shelter; K: Kuiseb Dune Complex.

SI Table 5. Data recorded on San digging sticks housed at Museum Africa (Fourie collection)

specimen number	total length	bevel type *	1st bevel length	2nd bevel length	bevel width	bevel thickness	bevel width 2 cm	flat face thick 2 cm	flat face width 4cm	flat face thick 4cm	weight (g)
1459	1072	d	72.49	69.49	20.24	19.74	17.45	8.43	19.84	11.68	233.00
1480	935	s	65.39	na	16.50	16.44	16.82	6.83	16.61	11.82	223.90
1461	1160	d	76.88	76.95	21.20	21.24	18.14	7.88	21.82	12.28	283.90
1462	1127	d	63.46	60.46	18.46	17.73	18.46	8.82	18.16	11.54	192.30
169A	903	d	65.38	63.22	17.74	16.60	17.59	5.88	18.58	8.04	147.70
2313	758	d	77.94	54.26	14.63	14.76	14.89	5.59	14.67	10.19	178.40
2996	996	s	108.00	na	22.49	24.15	16.39	8.91	21.75	12.42	405.90
169B	1031	d	54.42	53.36	16.13	16.16	16.87	6.58	16.64	9.96	147.60
1463	1799	d	91.69	78.64	23.85	20.59	22.14	8.63	24.22	11.26	458.70
2312	1386	d	106.42	88.67	20.92	19.01	18.64	5.35	20.56	7.74	259.50
2995	1300	s	214.00	na	31.47	34.01	16.89	9.14	23.92	12.75	877.90
2591	595	d	81.49	23.29	26.6	20.70	21.59	8.61	23.05	13.46	385.70
11166	955	s	155.00	na	30.88	31.33	24.82	7.94	28.33	10.97	787.40
1506	990	s	108.00	na	26.38	20.00	23.07	8.42	26.20	12.23	390.00

* d: double, s: single; measurements are given in mm; thick: thickness

SI Table 6. List of compounds identified in the pyrogram of the wood of the poison applicator and digging stick by Py(HMDS)-GC/MS analysis (acids and alcohols are detected as their TMS derivatives). C – carbohydrates, G – guaiacyl.

N°	Compound		N°	Compound	
1	phenol		29	1,4:3,6-dianhydro-α-D-glucopyranose	C
2	2-hydroxypropanoic acid		30	catechol (1,2-dihydroxybenzene)	
3	glycolic acid		31	m/z: 73, 129, 143, 213, 217	
4	hydroxymethyl-?-furaldehyde	C	32	3-hydroxy-2-(hydroxymethyl)-2-cyclopenten-1-one	C
5	furancarboxylic acid	C	33	*E*-4,5-dihydroxy-2-cyclopenten-1-one	C
6	hydroxymethyl-?- furaldehyde	C	34	5-hydroxy-2-(hydroxymethyl)-2H-pyran-4(3H)-one	C
7	3-hydroxypropanoic acid		35	m/z: 73, 255, 270	C
8	m/z: 73, 101, 115, 131, 159		36	levoglucosane	C
9	m/z: 59, 73, 115, 145, 188		37	4-hydroxybutanoic acid	
10	m/z: 73, 109, 139, 183, 198		38	levoglucosane	C
11	4-hydroxy-5,6-dihydro-(2H)-pyran-2-one	C	39	2-methyl-1,3-dihydroxybutane	
12	m/z: 73, 101, 116, 147		40	m/z: 73, 103, 185, 243, 258	
13	3-hydroxy-2-methyl-2-cyclopenten-1-one	C	41	1,2,3-trihydroxybenzene	C
14	2-hexenoic acid	C	42	m/z: 73, 147, 155, 273	

15	2-hydroxy-3-methyl-2-cyclopenten-1-one	C	43	dehydrated glucose	C
16	guaiacol	G	44	2-hydroxymethyl-5-hydroxy-2,3-dihydro-(4H)-pyran-4-one	C
17	1,3-dihydroxypropan-2-one		45	1,6-anhydro-D-galactopyranose	C
18	benzoic acid		46	1,2,4-trihydroxybenzene	C
19	m/z: 73, 103, 117, 147		47	1,6-anhydro-D-galactopyranose	C
20	m/z: 73, 217		48	m/z: 73, 129, 147, 191, 204, 217	C
21	hydroxy-3,4-dimethylcyclohexane	C	49	m/z: 73, 103, 147, 255, 345, 360	
22	2-methyl-3-hydroxy-(4H)-pyran-4-one	C	50	1,6-anhydro-ß-D-glucopyranose (levoglucosane)	C
23	glycerol		51	m/z: 73, 129, 147, 191, 204, 217	C
24	m/z: 73, 147, 198, 231		52	1,6-anhydro-ß-D-glucofuranose	C
25	2-furyl-hydroxymethylketone	C	53	vanillic acid	G
26	5-(hydroxymethyl)-2-furaldehyde	C	54	3-deoxy-D-ribo-hexono-1,4-lactone	C
27	4-hydroxy-5,6-dihydro-(2H)-pyran-2-one	C	55	3-deoxy-D-arabino-hexono-1,4-lactone	C
28	m/z: 73, 103, 129, 155, 170	C			

SI Table 7. List of compounds identified in the lipid fraction of the samples from the poison applicator by GC/MS analysis (acids and alcohols are detected as their TMS derivatives); 46a is a sample of the residue on the tip of the applicator, 46cr is a sample of residue collected from the middle of the piece.

N°	**Tr (min)**	**Compound**	**46a**	**46cr**
1	8.83	4-hydroxy-benzoic acid	✓	✓
IS1	9.13	hexadecane	✓	✓
2	9.76	dodecanoic acid (lauric)	✓	✓
3	9.98	m/z: 73, 191, 207, 221	✓	-
4	10.34	α,ω-octanedioc acid (suberic)	✓	✓
IS2	10.83	tridecanoic acid	✓	✓
5	11.01	vanillic acid	✓	-
6	11.36	α,ω-nonanedioc acid (azelaic)	✓	✓
7	11.98	tetradecanoic acid (myristic)	✓	✓
8	12.47	α,ω-decanedioic acid (sebacic)	✓	✓
9	12.76	pentadecanoic acid	✓	✓
10	12.89	hexadecanol	✓	✓
11	13.22	α,ω-undecanedioic acid	✓	-
12	13.42	*cis*-9-hexadecenoic acid (palmitoleic)	✓	✓

13	13.67	hexadecanoic acid (palmitic)	✓	✓
14	14.12	α,ω-dodecandioic acid	✓	-
15	14.72	octadecanol	✓	✓
16	15.29	*cis, cis*-9,12-octadecadienoic acid (linoleic)	✓	✓
17	15.36	*cis*-9-octadecenoic acid (oleic)	✓	✓
18	15.45	*trans*-9-octadecenoic acid (elaidic)	✓	-
19	15.70	octadecanoic acid (stearic)	✓	✓
20	17.36	eicosanol	✓	✓
21	17.77	n-tetracosane	✓	✓
22	18.31	12-hydroxy-*cis*-9-octadecenoic acid (ricinoleic)	✓	-
23	18.37	12-hydroxy-*trans*-9-octadecenoic acid (ricinelaidic)	✓	-
24	19.25	n-pentacosane	✓	✓
25	19.88, 20.11	m/z: 187, 383, 416	✓	-
26	20.32	n-hexacosane	✓	✓
27	20.79	docosanoic acid	✓	✓
28	21.03, 21.14	m/z: 73, 187, 317	✓	✓
29	21.28	n-eptacosane	✓	✓
30	21.77, 21.85	m/z: 187, 391, 427	✓	-
31	22.14	n-octacosane	✓	✓
32	22.49	tetracosanoic acid	✓	✓
33	22.93	n-nonacosane	✓	✓
34	23.66	n-triacontane	✓	✓
35	24.35	n-hentriacontane	✓	✓
36	24.61	cholesterol	✓	✓
37	25.94	ß-sitosterol	✓	tr

SI Table 8. Data on Kalahari San poison sticks housed at Museum Africa (Fourie Collection) and Border Cave piece

Specimen no.	length (cm)	width (mm)	thickness (mm)
928	47,7	6,15	6,18
2805	45,2	5,28	5,53
2804	32,7*	6,17	6,28
2607	18,4	6,16	6,29
632	49,6	6,59	7,32
535	49,5	6,27	6,31
712	38,5	7,2	6,77
2802	40,5*	5,91	5,65
Border Cave	8,294**	5,50	4,72
Border Cave	9,83**	5,36	4,70
Border Cave	8,825**	5,20	5,08
Border Cave	5,336**	4,35	4,22

* broken at one end; ** broken at both ends

SI Table 19. List of compounds identified in the lipid fraction of the extracts of samples 7 and 7* (lump of organic material) by GC/MS analysis (acids and alcohols are detected as their TMS derivatives).

N°	Tr (min)	Compound	N°	Tr (min)	Compound
1	8.58	acetophenone	25	19.91	docosanol
IS1	9.28	hexdecane	26	20.79	docosanoic acid
2	9.80	dodecanoic acid (lauric)	27	21.30	n-heptacosane
3	10.34	α,ω-octanedioc acid (suberic)	28	21.51	(ω-1)-hydroxy-eicosanoic acid
IS2	10.84	tridecanoic acid	29	21.80	tetracosanol
4	11.30	n-nonadecane	30	22.49	tetracosanoic acid
5	11.36	α,ω-nonanedioc acid (azelaic)	31	22.94	n-nonacosane
6	11.98	tetradecanoic acid (myristic)	32	23.35	hexacosanol
7	11.93	phtalate*	33	23.85	1,23-tetracosanediol
8	12.78	pentadecanoic acid	34	23.97	hexacosanoic acid
9	12.90	hexadecanol	35	24.35	n-hentriacontane
10	13.23	n-heneicosane	36	24.47	(ω-1)-hydroxy-tetracosanoic acid
11	13.85	hexadecanoic acid (palmitic)	37	24.71	octacosanol

12	14.60	heptadecanoic acid	38	25.14	1,25-hexacosanediol
13	14.75	octadecanol	39	25.27	octacosanoic acid
14	15.37	(9Z)-octadecenoic acid (oleic)	40	25.67	n-tritriacontane+ ß-amyrone + Δ^{18} friedelen-3-one
15	15.72	octadecanoic acid (stearic)	41	25.93	ß-amyrin + Δ^{18} friedelen-3-ol
16	16.45	n-tricosane	42	26.03	triacontanol + m/z: 189, 204, 483, 498
17	16.71	(ω-2)-hydroxy-hexadecanoic acid	43	26.30	lupeol
18	16.95	(ω-1)-hydroxy-hexadecanoic acid	44	26.39	cycloartanol
19	17.19	nonadecanoic acid	45	26.78	triacontanoic acid
20	17.38	eicosanol	46	27.79	dotriacontanol
21	18.61	eicosanoic acid	47	28.25	m/z: 143, 481, 496
22	19.25	n-pentacosane	48	29.96	m/z: 189, 203, 320
23	19.41	(ω-2)-hydroxy-octadecanoic acid	49	30.28	tetratriacontanol
24	19.58	(ω-1)-hydroxy-octadecanoic acid	50	30.65	m/z: 146, 189, 218, 367

Figures

SI Figure 5. Longitudinal scraping marks on the split surface of a tusk from 2WA (**top left**); grinding and scraping on a tusk from the same layer (**top right**); grinding on the split surface and the tip of a tusk from 2BS Lower C (**bottom**). Notice the natural occlusal wear pattern on the lower aspect of the tusk (**bottom centre**), and polishing and rounding of the tip (**bottom right**). Scale = 1 cm.

SI Figure 6. Longitudinal scraping on the split surface of a tusk from 2BS Lower C (**top left**); scraping and grinding on a burnt tusk fragment from 1WA (**top right**); Scraping marks and transverse deep incisions, probably to facilitate hafting, on a point made of a tusk from 1BS Lower B-C (**bottom left**); Longitudinal scraping on the occlusal wear facet on a tusk from the same layer (**bottom right**). Scale = 1 cm.

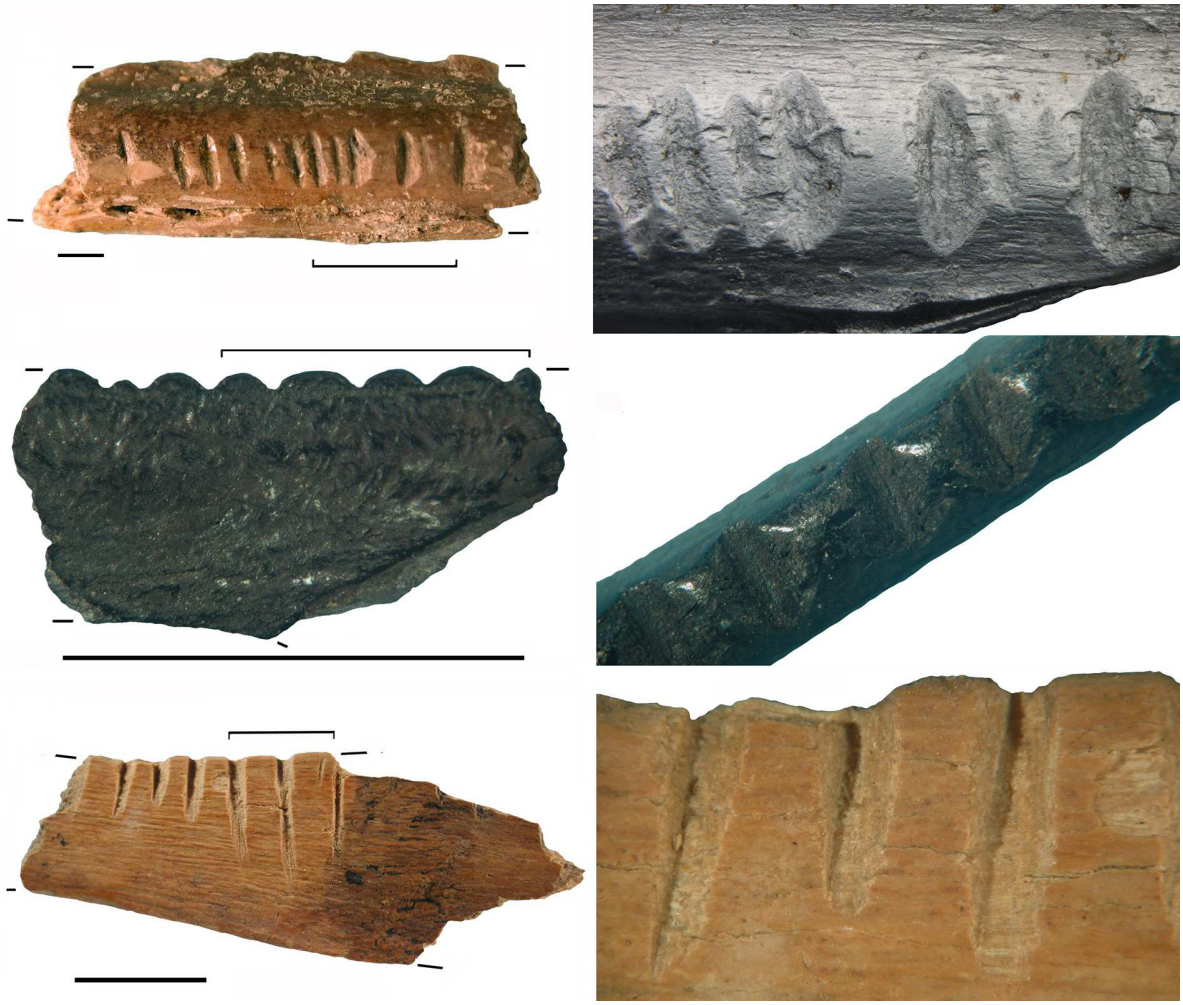

SI Figure 7. Notched bones from layers 2WA (**top**) and 1WA (**centre and bottom**). Note the evenly spaced notches and highly polished elevations between them on the burnt piece. One close-up (**top right**) was taken in transmitted light on a resin replica. The lack of patina on the specimen at the bottom is probably due to invasive cleaning. Scale = 1 cm.

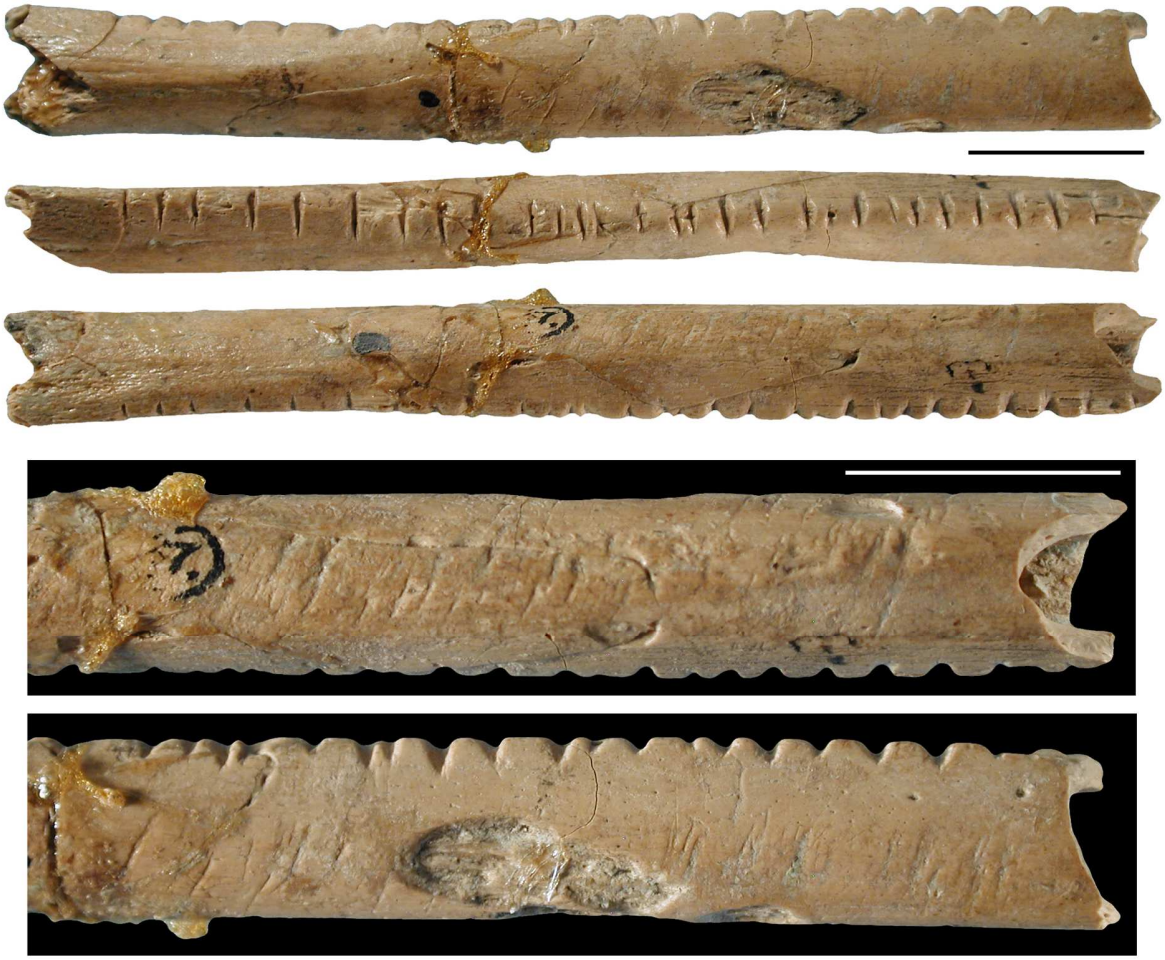

SI Figure 8. Baboon fibula from 1BS Lower B-C presenting an incomplete sequence of 29 notches along the interosseous crest, and oblique incisions on the other aspects (**top**). Note the changes in the section of the notches (**bottom**) indicating the use of different cutting edges. Scale = 1 cm.

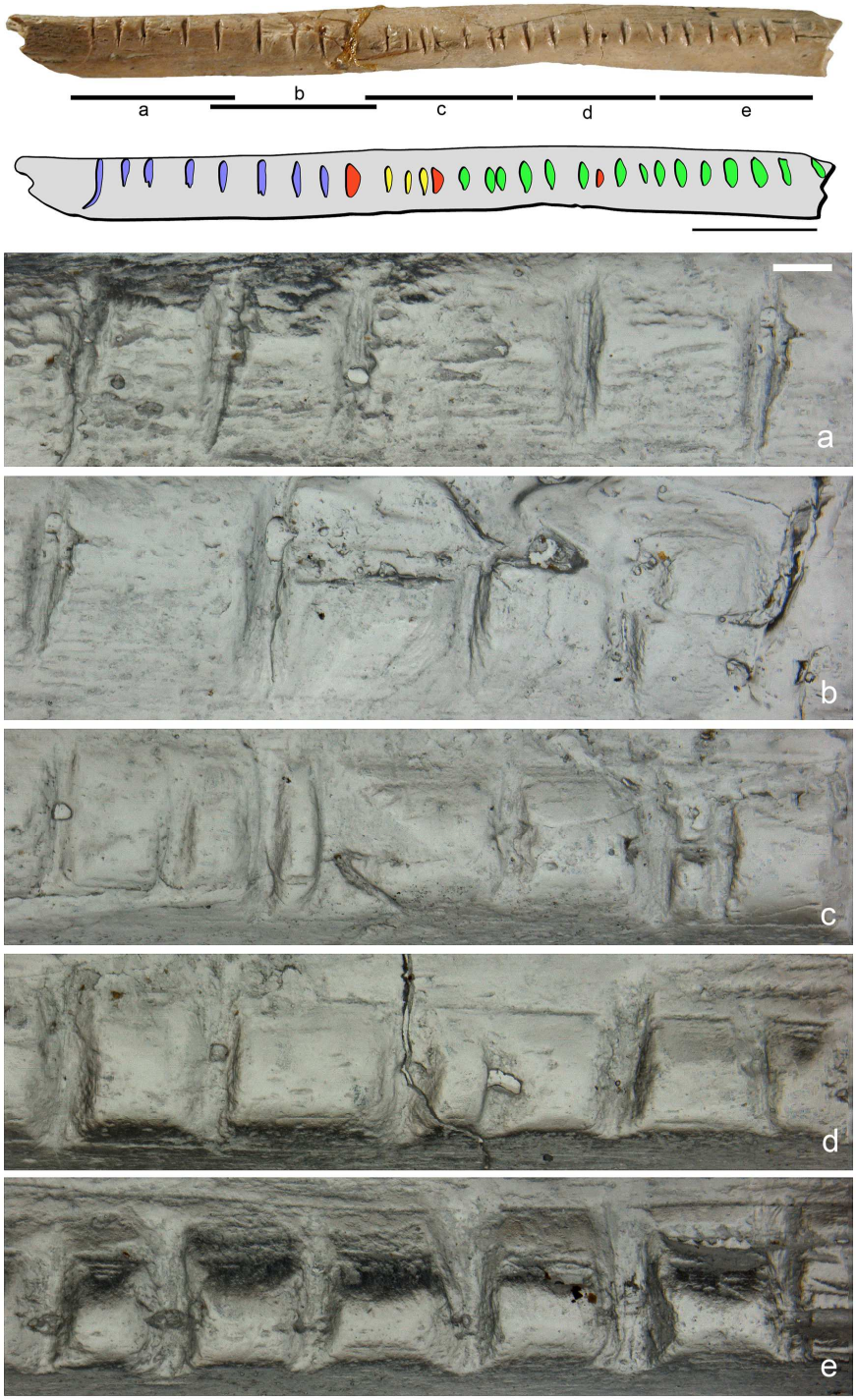

SI Figure 9. Photo and interpretive drawing of the notched aspect of the baboon fibula from 1BS Lower B-C with notches made by the same tool shown in the same colour (**top**). Letters indicate segments enlarged to highlight the morphology of notches on resin replicas photographed in transmitted light (**bottom**). Scale = 1 cm (top) and 1 mm (bottom).

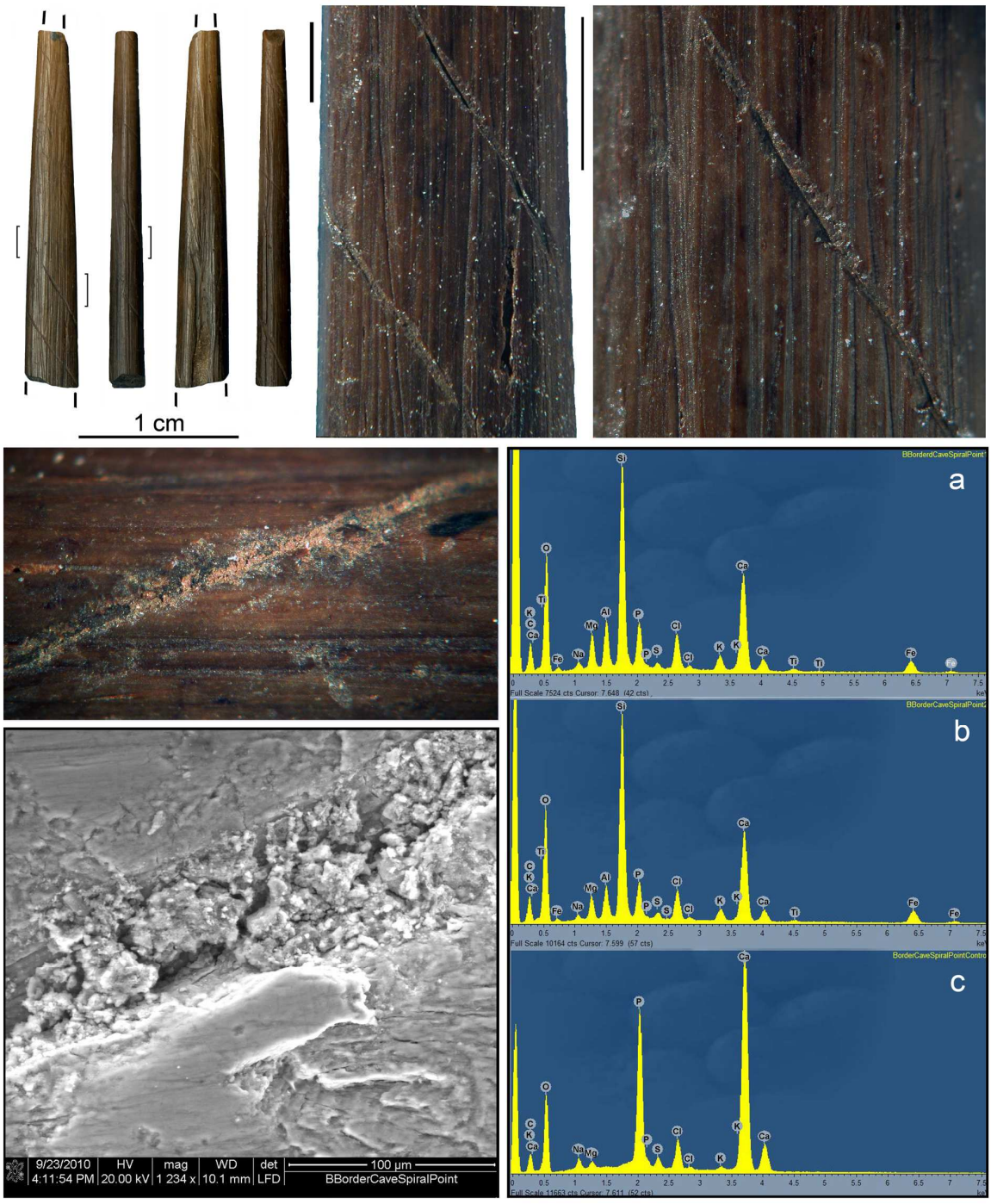

SI Figure 10. Thin bone point from 1WA shaped by scraping and decorated with a delicate spiralling incision filled with red pigment (**top and bottom left**). Comparative energy dispersive x-ray analysis of two spots on the pigment (a, b) and a control area on the adjacent bone surface (c) indicates that the pigment is made of C, Si, Fe, Mg, Al, and Ti, suggesting the use of an iron-rich clay retaining an organic content. Vertical scales = 1 mm.

SI Figure 11. Tip of a broken and burnt awl from 1WA (**left**) showing evidence of re-sharpening by grinding (**close-up, left**), scraping and polishing through use (**close-up, centre**), and longitudinal breakage (**close-up, right**). Scale left = 1 cm; scale right = 1 mm.

SI Figure 12. Burnt bone point from 1BS Lower B-C in three pieces (**left**) shaped by intense scraping (**right**). Scale left = 1 cm; scale right = 1 mm.

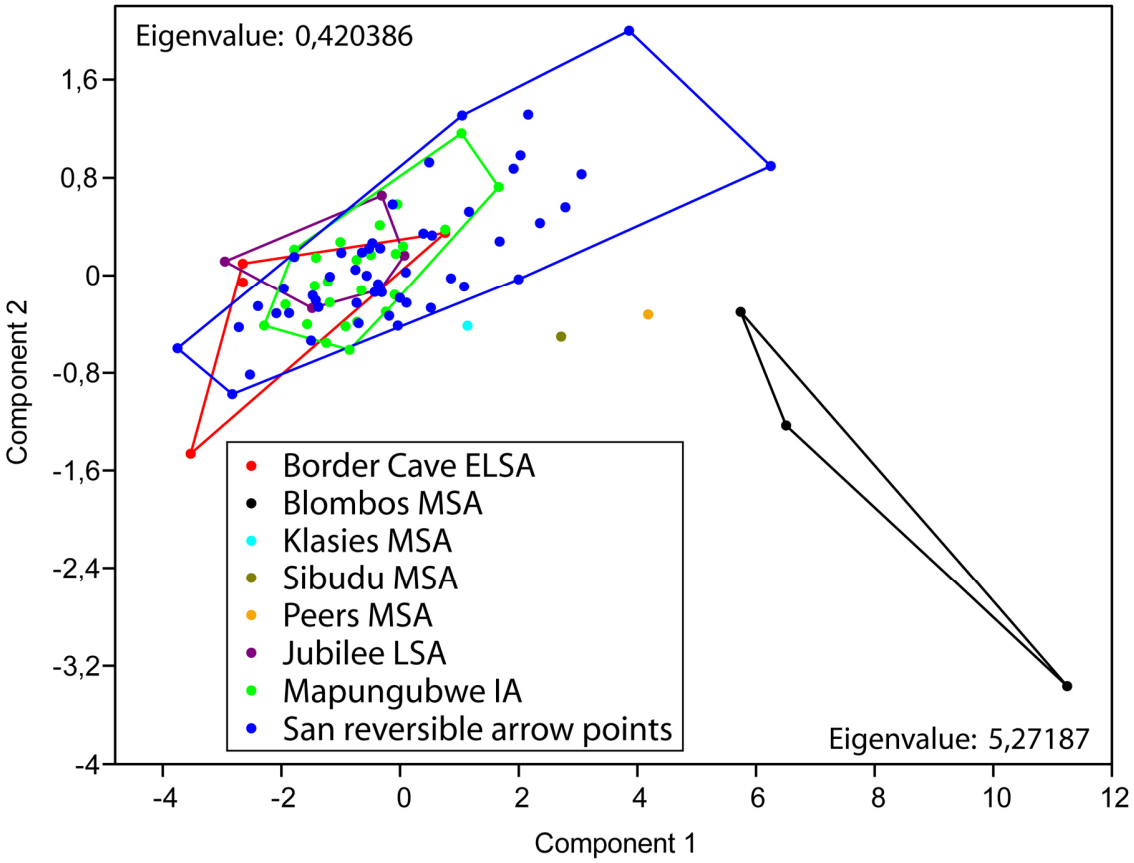

SI Figure 13. Principal Component Analysis of the thickness and width of San bone arrow points used with poison, Iron Age (IA), Later Stone Age (LSA), and Middle Stone Age (MSA) bone points at 5, 10 and 30 mm from the tip (see Table S2).

SI Figure 14. Ostrich eggshell beads from 1WA and 1BS Lower B-C (**top**); close-up view showing the conical (**centre middle and left**) and cylindrical (**centre middle and right**) morphology of perforations; beads homogeneously blackened by heating (**bottom**).

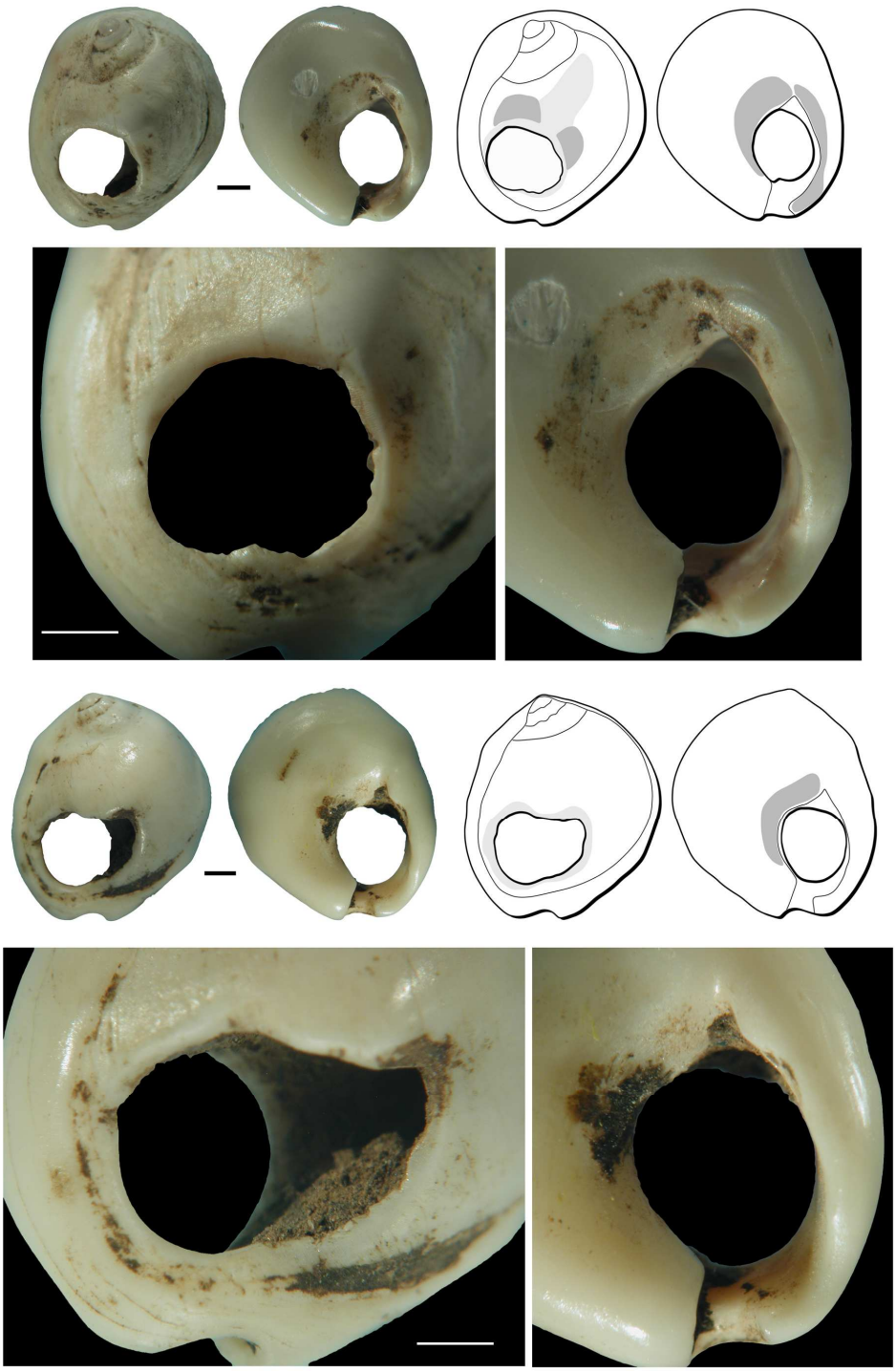

SI Figure 15. *Nassarius kraussianus* shell beads from 1WA (**bottom**) and 1BS Lower B-C (**top**). Smoothing and use wear facets are indicated in the drawings with pale and dark grey respectively. Close-up views show use wear traces around the perforation (**left**) and the aperture (**right**). Scales = 1 mm.

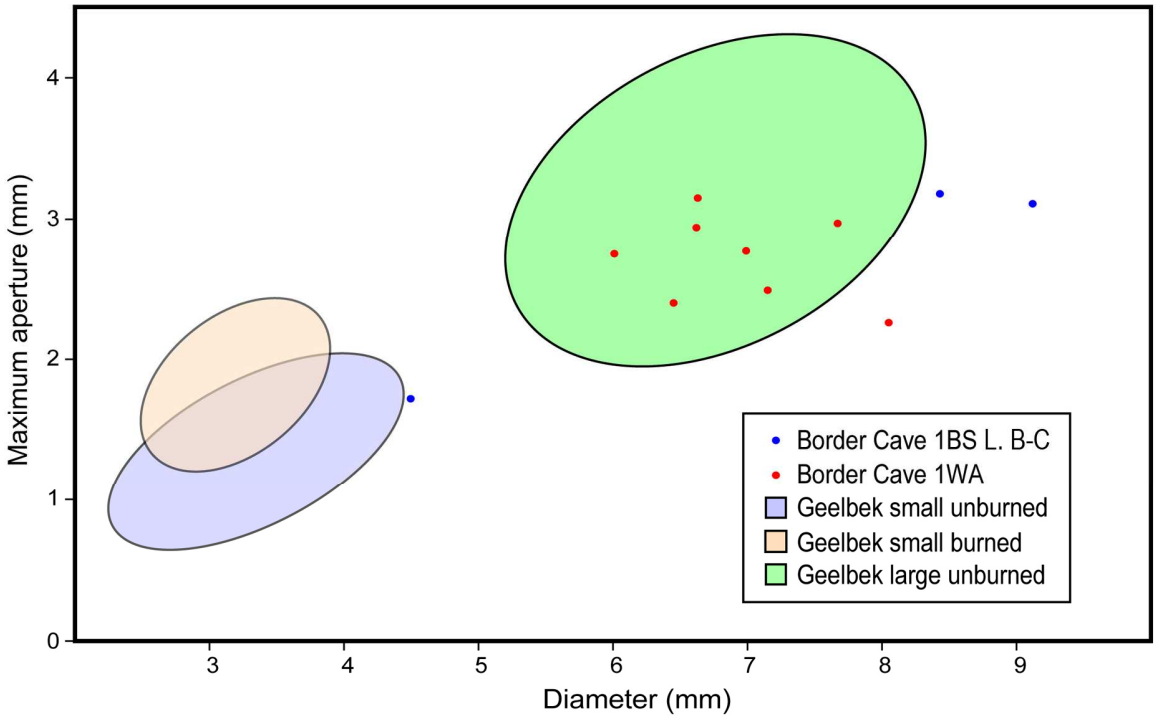

SI Figure 16. Scattergram plotting the diameter against the internal aperture of OES beads from Border Cave layers 1WA and 1BS Lower B-C, and the confidence ellipses for small (<5 mm) and large (>5 mm) OES beads from the Geelbek Dunes LSA sites, Western Cape; data after (26).

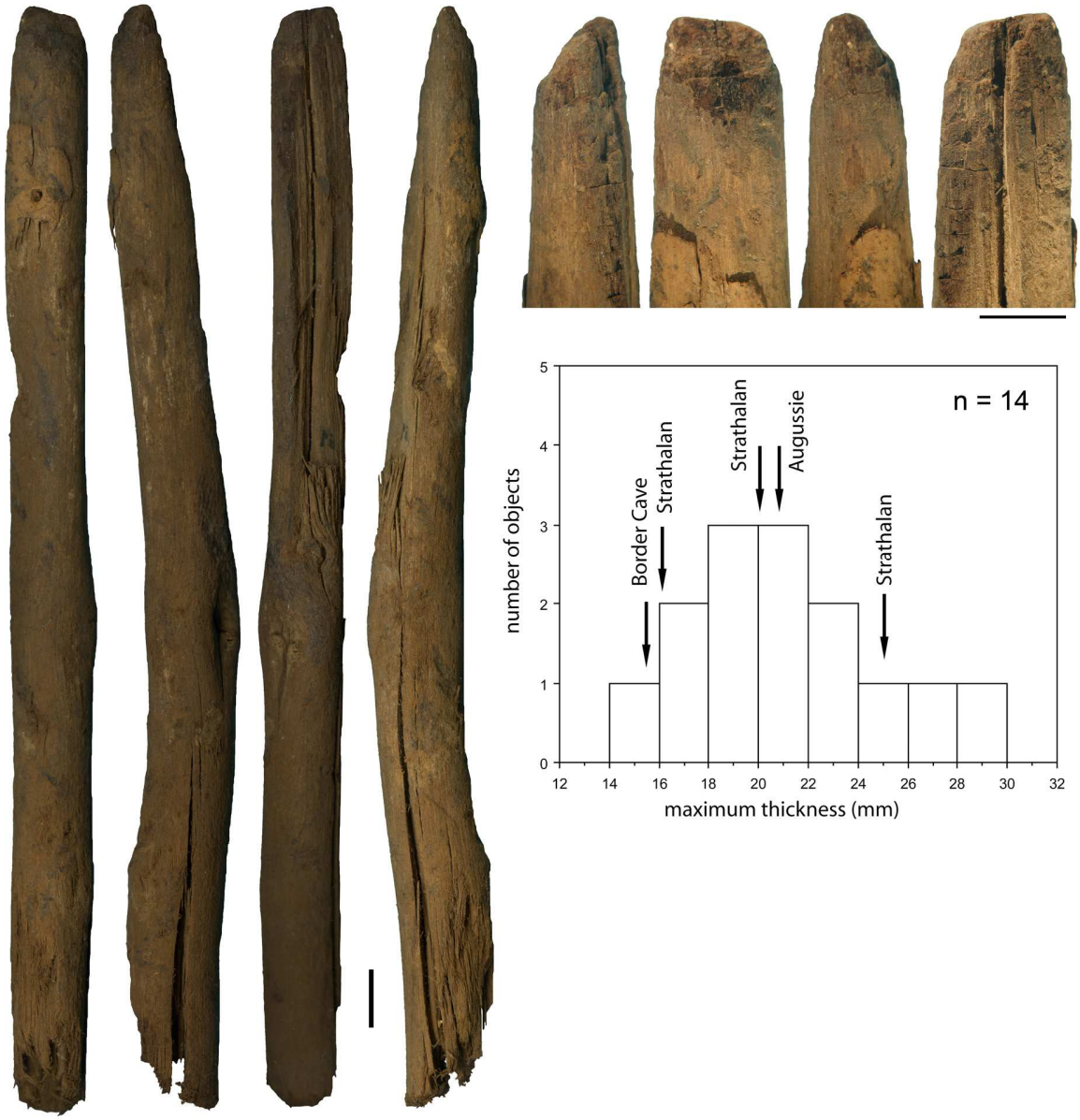

SI Figure 17. Wooden digging stick from 1BS Lower B-C (**left**); close-up view of the tip (**top right**); histogram of the thickness of San digging sticks, with arrows indicating the thickness of digging sticks from LSA sites and Border Cave. Scales = 1 cm.

SI Figure 18. Kalahari San digging sticks from the Fourie Collection (Museum Africa, Johannesburg) analysed in the framework of this study (**top**); morphology of utilised ends bearing similarity to the Border Cave specimen (**bottom**). Scales = 1 cm.

2 mm
a
f
v
r
v
p
50 µm
b
g
v
v
50 µm
c
r
f
v
20 µm
d
Rp
Ru
200 µm
e
r
f
g
v
50 µm
f

SI Figure 19. **a**: rounded tip of the digging stick with hardened resiniferous exudates seen as red or dark streaks; **b**: transverse section (TS) of the digging stick showing vessels (v) in short radial multiples, narrow rays (r). The amorphous brown (dark) substance obscuring some of the cells is probably resin or gum originating from the vessels or ray cells. Fibres (f); scattered parenchyma cells (p); **c**: TS at higher magnification to show details of the vessel arrangement, with resin or gum (g); **d**: TS axial parenchyma is diffuse – seen as single scattered thin-walled empty cells. Fibres have thick walls and there are examples of some that have become detached from the middle lamella. Note the biseriate ray comprising long cells (upright in radial longitudinal view (r); **e**: radial longitudinal section of the ray showing the upright to square cells (Ru) and procumbent body cells (Rp). Crystals are seen as shiny white flecks; **f**: poison applicator, TS with the same features as the digging stick.

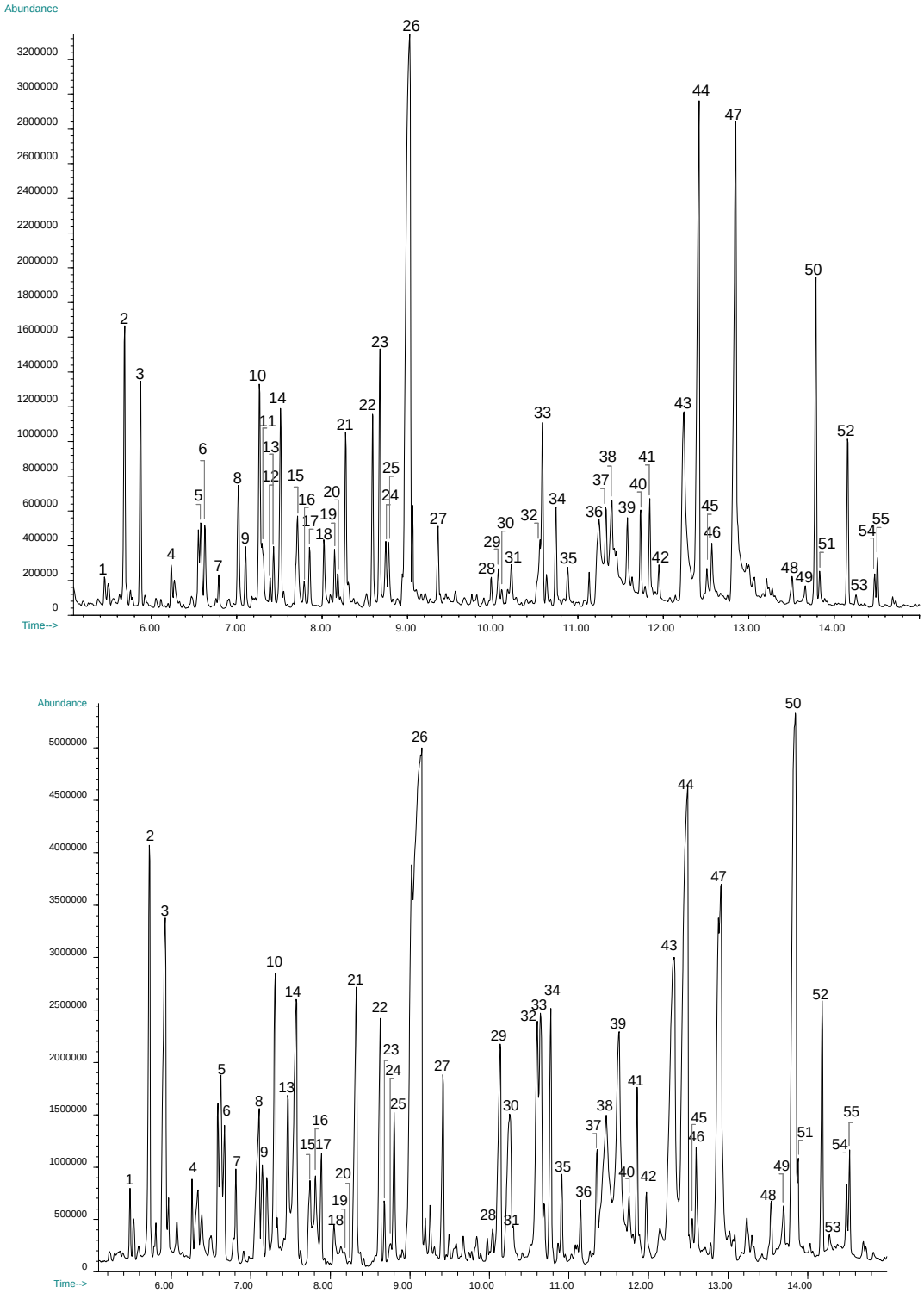

SI Figure 20. Py(HMDS)-GC/MS profiles of sample 46c from the wood of the poison applicator (**top**) and sample 47a from the digging stick (**bottom**).

SI Figure 21. Three aspects of the four pieces comprising the poison applicator from 1BS Lower B-C (**top left**); close-up view of the incisions on the surface (**top right**); residue at the end of one piece analysed in this study (**bottom**). Scales at the top = 1 cm; scales at the bottom = 1 mm.

SI Figure 22. Kalahari San poison applicators housed at Museum Africa, Johannesburg (Fourie Collection). Note the lumps of organic compounds used for hafting (yellow) and poisoning (black) arrow points, and the notching to prevent slippage of the material. Scales = 1 cm.

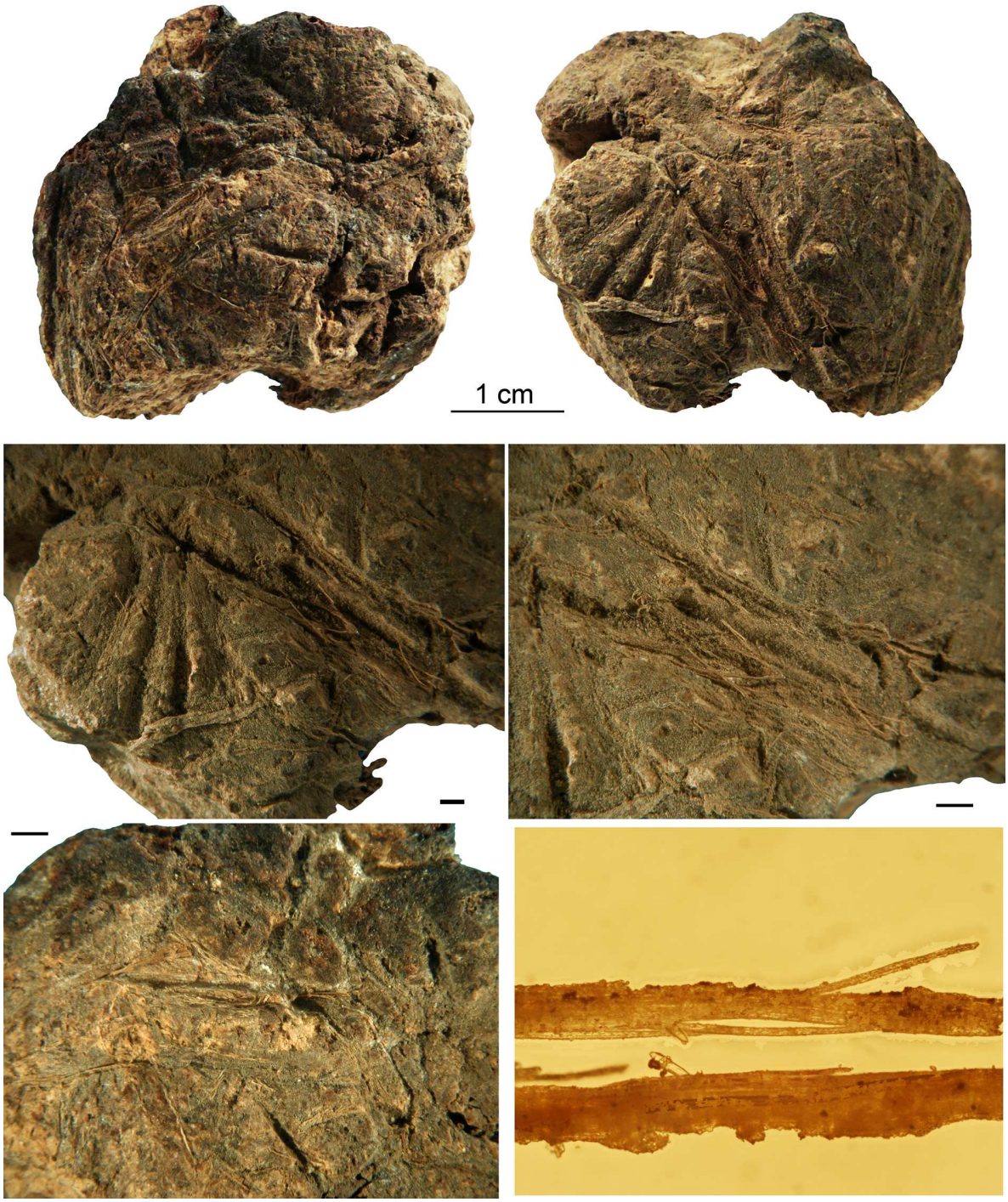

SI Figure 23. Lump of organic material from 1BS Lower B-C (**top**); close-up views of grooves resulting from binding, and still filled with remnants of vegetal twine (**centre and bottom left**); photo of two of the fibres (400x), probably from the inner bark of a woody plant (**bottom right**). Scales = 1 mm.

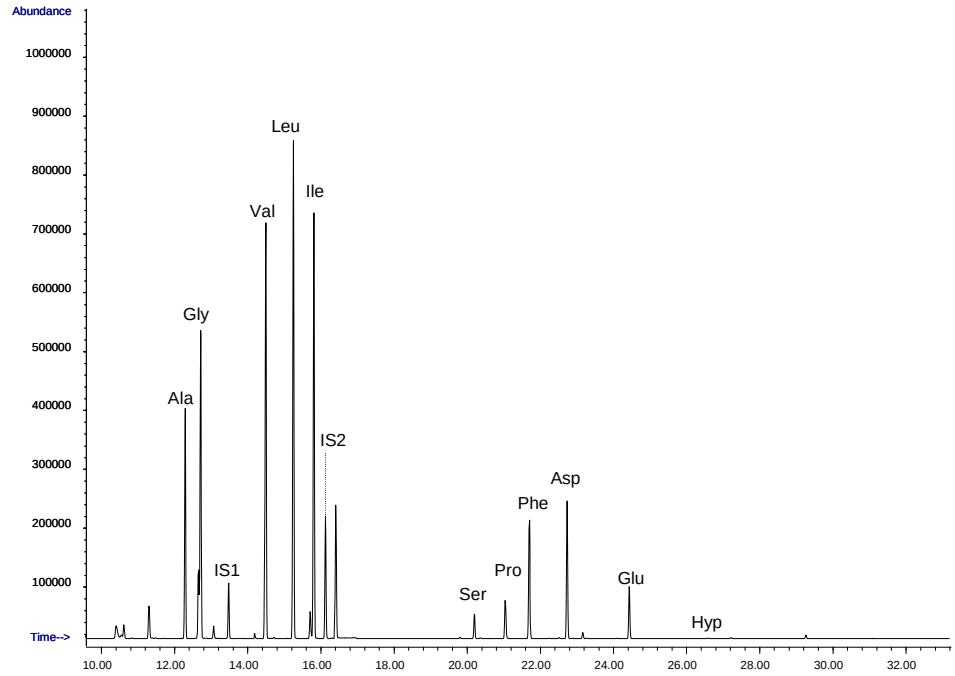

SI Figure 24. Gas chromatogram of the proteic fraction of a sample from the bound organic material (sample 7*) acquired in SIM mode; (Ala = alanine, Gly = glycine, Val= valine, Leu = leucine, Ile = isoleucine, Pro = proline, Phe = phenylalanine, Asp = aspartic acid, Glu = glutammic acid, Hyp = hydroxyproline, IS1 = hexadecane, IS2 = norleucine).

Materials and Methods

Microscopic and morphometric analysis

Organic artifacts from layers 2WA, 2BS Lower C, 1WA, and 1BS Lower B-C were examined with an Olympus SZX16 stereo microscope at magnifications between 4 and 40x to document natural and anthropogenic modifications, and the presence of residues. Selected objects were analysed with a Quanta 400 ESEM equipped with an Energy Dispersive Spectroscopy facility at a voltage of 15 kv. Identification of shaping techniques and use wear on bone artifacts is based on identification of non-human modifications (30-32), experimental replication of traces of manufacture and use (33-42), ethnographic collections (43-44) and comparative analysis of well preserved Middle Stone Age, Upper Palaeolithic and Later Stone Age artifacts (45-47). In particular we have examined the

occlusal wear on warthog and bushpig lower canines housed at the Bernard Price Institute for Palaeontological Research, University of the Witwatersrand, to characterise the type and orientation of striations on these areas.

The San bone arrow points that we have analysed (Table S2) are part of the Fourie Collection, accumulated between 1916 and 1928 by Dr. Louis Fourie in the Kalahari and now housed at Museum Africa, Johannesburg (48). We have focused exclusively on Type 3 bone arrow points, described by Goodwin (49) as long, slender and lens-shaped, with a cone-shaped tip. They are always bound to stout lens-shaped linkshafts. The bone arrow head is completely encrusted with poison, so when not in use, is reversed in the reed. This type was universally used in southern Africa by San and in the LSA (50). Data on MSA points come from the literature and direct analysis of the material (45, 46). Data on LSA and Iron Age bone points, housed in the Department of Archaeology, University of the Witwatersrand, and University of Pretoria respectively, were directly recorded at those institutions.

Metric data were collected on all objects with digital callipers and for the points, recorded variables included, whenever possible, the maximum width and thickness as well as these same measurements at 5, 10 and 30 mm from the tips of all the specimens studied.

Resin replicas of the tips and modified areas were moulded using Coltène® President light body high resolution dental impression material, and cast in M resin (Plastomax, South Africa). Replicas were observed and photographed in transmitted light with a Leica Z6 APOA microscope with a multifocus module.

Analysis of marine shells was based on previous work that assessed the artifactual nature of Middle Stone Age perforated shells, incorporating taphonomic analysis, experimental replication of perforation and use, and the significance of size variability (51). Length and width of shells, and the size of perforations was also recorded. Ostrich eggshell beads were studied according to criteria suggested by (26). In particular we recorded the colour, perforation technique, evidence of burning, polish, width, maximum and minimum diameter of the bead and the aperture. Wooden artifacts were analysed in search of modifications experimentally produced on wood by stone tools (52, 53) and heating (54). We compared traces on the artifacts from Border Cave with those described from the few Palaeolithic sites from Africa (55-57), Europe (54, 58) and the Near East (59) that have yielded wooden artifacts. We also compared the Border Cave specimens with wooden artifacts from the Fourie Collection housed at Museum Africa in Johannesburg, South Africa. On digging sticks from this collection we recorded the presence of a single or double bevel, the length of the bevel, the width

and thickness of the functional area at 2 and 4 cm from the tip, and the maximum and minimum diameter of the artifact. The same variables were recorded on the specimen from Border Cave and gathered from the literature for LSA digging sticks (60, 61). On arrow shafts and wooden sticks used as poison applicators we recorded length, and maximum and minimum diameter. On the latter we also recorded the presence of notching and residues.

Chemical analyses

Residues on a broken notched stick (samples 46a and 46cr), samples of a purported lump of beeswax, (samples 7 and 7*) and a digging stick (sample 47a) (Table 1) were submitted to an analytical procedure using Gas Chromatography/Mass Spectrometry (GC/MS) to identify lipids, waxes, proteins, resinous materials and saccharides (21, 22, 23) and Pyrolysis-Gas Chromatography/Mass Spectrometry (Py(HMDS)-GC/MS) to characterise the wooden material (62).

Reagents

All the solvents were Baker HPLC grade and were used without any further purification. Trifluoroacetic acid (99% purity) and anhydrous pyridine were from Fluka (Milan, Italy). Ethanethiol (ETSH; 99.5%), sodium azide (NaN3; 99.5%), *N*,*O*-bis(trimethylsilyl)trifluoroacetamide (BSTFA) with and without 1% trimethylchlorosilane, *N*-*tert*-butyldimethylsilyl-*N*methyltrifluoroacetamide (MTBSTFA) with 1% trimethylchlorosilane, 1,1,1,3,3,3-hexamethyldisilazane (HMDS, 99.9%) and triethylamine were from Sigma-Aldrich. The following solutions, apart from those for the amino acids, were prepared by weighing pure substances and were used as standards: (i) amino acid solution in 0.1 M HCl (Sigma-Aldrich) and containing 12.5 µmol/mL of proline (Pro) and hydroxyproline (Hyp) and 2.5 µmol/mL of aspartic acid (Asp), glutamic acid (Glu), alanine (Ala), arginine, cysteine, phenylalanine (Phe), glycine (Gly), hydroxylysine, isoleucine (Ile), histidine, leucine (Leu), lysine (Lys), methionine (Met), serine (Ser), tyrosine (Tyr), threonine, and valine (Val); (ii) solution of fatty and dicarboxylic acids in acetone, containing lauric acid (0.24 mg/ g), suberic acid (0.27 mg/g of Su), azelaic acid (0.28 mg/g of A), myristic acid (0.25 mg/g of My), sebacic acid (0.3 mg/g of Se), palmitic acid (0.25 mg/g of P), oleic acid (0.51 mg/g of O), stearic acid (0.51 mg/g of S) [all acids (purity >99%) from Sigma-Aldrich]; (iii) norleucine solution in bidistilled water (Sigma-Aldrich; purity 99%, 138.66 µg/g) was used as a derivatization internal standard for amino acids; (iv) tridecanoic acid solution in isooctane (Sigma-Aldrich; purity 99%, 135.48 µg/g) was used as a lipid-resinous fraction derivatization internal standard; (v) hexadecane solution in isooctane (Sigma-

Aldrich; purity 99%, 80.34 µg/g) was used as an injection internal standard; (vi) monosaccharides and uronic acids solution in bidistilled water containing D-(+)-galactose (0.1 mg/g), L-(-)-fucose (0.1 mg/g), L-(+)-arabinose (0.1 mg/g), L-(-)-ramnose (0.1 mg/g), L-(-)-mannose (0.1 mg/g), D-(+)-xylose (0.1 mg/g), D-(+)-glucose (0.1 mg/g), D-glucuronic acid (0.1 mg/g), D-galacturonic acid (0.1 mg/ g) monohydrate; and (xi) mannitol in bidistilled water (0.1 mg/g) was used as a derivatisation internal standard for aldoses and uronic acids. All monosaccharides and uronic acids (purity 99%) were from Sigma-Aldrich (Milan, Italy). All standard solutions were stored at 4°C.

Raw materials

Beeswax was purchased from a local beekeeper (Sarzan, Italy); castor oil from *Ricinus communis* was supplied by Zeta Farmaceutici s.p.A. (Sandrigo, Vicenza, Italy). Branches and leaves of *Euphorbia tirucalli* and *Securinega virosa* were collected in South Africa; wood and branches of both plants were also provided by the Herbarium of the University of Witwatersrand.

Analytical procedure and instrumentation

The sample treatment, already described in the literature (21, 22), needed prior to GC/MS analysis, consists of a multistep chemical pre-treatment based on the ammonia extraction of proteins and polysaccharide materials in order to separate them from lipid and resinous materials. The extraction is then followed by the separation and purification of proteinaceous and polysaccharide materials before hydrolysis. Lipids and resins are saponified/salified separately. Three fractions are generated, derivatised with silylating agents and analyzed separately by GC/MS, thus enabling a quantitative analysis to be performed.

A microwave oven model (MLS-1200 MEGA Milestone, FKV, Sorisole, Bergamo, Italy) was used for the hydrolysis of proteins and peptides, and the saponification/salification of glycerolipid, waxy, and resinous materials.

The GC/MS instrumentation consists of a 6890N Network GC System (Agilent Technologies, Palo Alto, CA, USA) equipped with a PTV injector and coupled to a 5973 MS detector with quadrupole analyser. The pyrolyser coupled to the GC/MS was a 5150 CDS Pyroprobe 5000 Series pyrolyser with a platinum filament. MS was set with an electron impact ionisation (EI, 70 eV) in positive mode, an ion source temperature at 230°C, a scan range of 50-700 m/z, and an interface temperature of 280°C. GC separation was performed using a HP-5MS column (J&W Scientific, Agilent Technologies: stationary phase 5% phenil–95% methylpolysiloxane, 30 m length, 0.25 mm i.d., 0.25 m film thickness) connected to a deactivated fused silica precolumn (J&W Scientific,

Agilent Technologies: 2 m length, 0.32 mm i.d.). GC conditions for the lipid-resinous fraction involved the use of the PTV injector in splitless mode at 300°C; the chromatographic oven was programmed at 80° C for 2 min isothermal, 10°C/min up to 200°C, 4 min isothermal, 6°C/min up to 280°C, 40 minutes isothermal; constant He flow 1.2 ml/min, injector temperature 280°C. GC conditions for the proteic fraction involved the PTV injector used in splitless mode at 220°C; the chromatographic oven was programmed with an initial temperature of 100°C, isothermal for 2 min, then 4°C/min up to 280°C, and 280°C isothermal for 15 min. GC conditions for the saccharide fraction involved the PTV injector used in splitless mode at 250°C; the chromatographic oven was programmed at 50°C isothermal for 2 min, 5°C/min up to 190°C, 190°C isothermal for 20 min 5°C/min up to 280°C, and 280°C isothermal for 15 min. Pyrolysis was carried out for 20s at 550°C using a platinum coil probe and quartz sample tubes. 40–60 µg of each sample and hexamethyldisilazane (5 µL) were inserted in the centre of the pyrolysis quartz tube with glass wool, and then placed on the pyrolysis coil filament. Py-GC interface temperature was set at 180°C. Chromatographic parameters were initially 31°C, 8 min isothermal, 10°C min-1 to 240°C, 3 min isothermal, 20°C min-1 to 300°C, 30 min isothermal (62, 63, 64). Structural assignments are based on literature data, NIST and Wiley mass spectra libraries and spectra interpretation.

Botanical analysis

Very small portions of the wooden digging stick and poison applicator were cut from the archaeological specimens, photographed with an Olympus SZX16 microscope and Olympus SC30 digital camera. Then the pieces were embedded in resin and thin sections were made of the transverse sections because of the small size of the samples. The thin sections were studied and photographed under a Zeiss Axiophot petrographic microscope at 400x magnification, and photographed. Descriptions follow the recommendations of the IAWA Committee and identification has been made using the Insidewood online database and key (65, 66, 67).

Ostrich eggshell bead dating

The dating of this sample was undertaken at the Leibniz Labor für Altersbestimmung und Isotopenforschung, Christian-Albrechts-Universität, Kiel. To remove adhering dust and detrital carbonate as well as organic surface coating the eggshell sample was first cleaned with 30% H_2O_2 in an ultrasonic bath, followed by a second cleaning step with 15% H_2O_2 in an ultrasonic bath. The

sample CO_2 was liberated from the sample with 100% phosphoric acid at 90°C. The sample CO_2 was reduced with H_2 over 2 mg of Fe powder as catalyst, and the resulting carbon/iron mixture was pressed into a pellet in the target holder.

The ^{14}C concentration of the sample was measured by comparing the simultaneously collected ^{14}C, ^{13}C, and ^{12}C beams of the sample with those of Oxalic Acid standard CO_2 and pre-Eemian foraminifera background material. The conventional ^{14}C age was calculated according to (68), with a $\delta^{13}C$ correction for isotopic fractionation based on the $^{13}C/^{12}C$ ratio measured by our AMS-system simultaneously with the $^{14}C/^{12}C$ ratio (note: this $\delta^{13}C$ includes the effects of fractionation during graphitization and in the AMS-system and, therefore, cannot be compared with $\delta^{13}C$ values obtained per mass spectrometer on CO_2). For the determination of measuring uncertainty (standard deviation σ) we observe both the counting statistics of the ^{14}C measurement and the variability of the internal results that together make up one measurement. The larger of the two is adopted as measuring uncertainty. To this we add the uncertainty connected with the subtraction of our "blank". The quoted 1σ uncertainty is thus our best estimate for the full measurement and not just based on the counting statistics. We did not apply any reservoir age correction as the local value is unknown. The sample reported here gave enough carbon and produced sufficient ion beam during the AMS measurement. The $\delta^{13}C$ value is in the range previously reported by (69) and (70).

Poison applicator and digging stick dating

The dating of this sample was undertaken at the Oxford Radiocarbon Accelerator Unit, University of Oxford. The result is a conventional radiocarbon age BP (68) and uncalibrated in radiocarbon years BP (Before Present – AD 1950) using the half life of 5568 years. Isotopic fractionation has been corrected for using the measured $\delta^{13}C$ values measured on the AMS. The quoted $\delta^{13}C$ values were measured independently on a stable carbon isotope mass spectrometer (to ±0.3 per mil relative to VPDB). For details of the chemical pretreatment, target preparation and AMS measurement see (71) and (72). A calibration plot showing the calendar age ranges, was generated using the Oxcal computer program (v4-1) of (14), using the 'INTCAL09' dataset (73).

Beeswax dating

The dating of this sample was undertaken at the Oxford Radiocarbon Accelerator Unit, University of Oxford. The result is a conventional radiocarbon age BP of 35,410 ± 360 BP (68). The sample is

given an OxA-W- prefix because it was pretreated outside Oxford (Kiel) and combusted, graphitized and AMS dated in Oxford. Isotopic fractionation has been corrected for using the $\delta^{13}C$ value measured on the AMS. The quoted $\delta^{13}C$ values were measured independently on a stable carbon isotope mass spectrometer (to ±0.3 per mil relative to VPDB). For details of the chemical pretreatment, target preparation and AMS measurement see (72) and (73). A calibration plot showing the calendar age ranges, was generated using the OxCal computer program (v4-1) of (14), using the 'INTCAL09' dataset (74).

Bayesian modelling of C14 ages

We used OxCal 4.1 (14) to perform a Bayesian modelling analysis on radiocarbon ages from multiple levels at Border Cave (Fig. S2). We grouped the ages within six separate phases reflecting the principal stratigraphic upper units of the site (2 BS Lower A, 2 BS Upper, 1WA, 1BS Lower B, 1BS Lower C, 1BS Lower A). We excluded radiocarbon ages associated with levels 2BS Lower B and 2BS Lower C because they fall outside the range of the IntCal09 calibration curve. We also did not model five AMS ages (Fig. S1) obtained on objects from 1BS Lower B-C without a sub-level attribution. We included a boundary between each stratigraphic unit and assume an unordered distribution of likelihoods within each successive phase. We used fM (fraction modern) values corrected for background given by (13) and the radiocarbon dates from the Pretoria Radiocarbon Laboratory in the model. In an effort to identify measurement data (i.e., radiocarbon ages) that did not agree with the model (i.e., outliers), we used outlier detection analysis to measure the overlap between the likelihoods and posterior distributions (14, 75). We ran an initial Bayesian model using all the radiocarbon ages shown in Fig. S1, with the exception of determinations approaching the maximum limit of the INTCAL09 calibration curve (76). Outliers in the model are down-weighted with respect to the probability that they are outlying. Two determinations yielded higher outlier posterior probabilities (Pta-4700 (19%) and Pta-4706 (11%)); the remainder were 4-5%, which was the same level as the prior outlier probability ascribed. The age model is shown in Figure S2. Repeat iterations of the model resulted in similar results. Determinations from 2BS UP are dominated by results that are close to or beyond the INTCAL09 calibration curve and these should be viewed as minimum ages within the constraints of this model. We tested the sensitivity of the model to the inclusion and exclusion of the determinations from 2BS and the start and end boundaries for levels above, and found that it made little difference. In Figure S3 we show a summary of the key

chronometric information for levels 1WA, 1BS Lower C and 1BS Lower B in the form of summed probability distributions, which illustrates the range of the posterior (modelled) data for these archaeological horizons. Each distribution fits within the period 42-44 ka cal BP. Our analysis shows that Level 1WA starts between 44.2–43.0 ka cal BP (at 68.2% probability) and lasts for ~1300 years (at 68.2% prob.). Level 1BS Lower C starts afterwards at 43.0–42.5 ka cal BP. Level 1BS Lower C and B appear to be brief occupations with intervals of 0–350/400 years, respectively (Figure S4). The end of 1BS Lower B is equivalent to 42.5–41.9 ka cal BP.

References

1. Cooke H, Malan B, Wells L (1945) Fossil man in the Lebombo Mountains, South Africa: The Border Cave, Ingwavuma District, Zululand. *Man* 45:6–13.
2. Beaumont P (1973) Border Cave - A Progress Report. *S Afr J Sci* 69:41-46.
3. Beaumont P, Miller G, Vogel J (1992) Contemplating old clues to the impact of future greenhouse climates in South Africa. *S Afr J Sci* 88:490–498.
4. Butzer K, Beaumont P, Vogel J (1978) Lithostratigraphy of Border Cave, KwaZulu, South Africa: a Middle Stone Age Sequence Beginning c. 195,000 B.P. *J Archaeol Sci* 5(4):317–341.
5. Grün R, Beaumont P, Tobias P, Eggins S (2003) On the age of Border Cave 5 human mandible. *J Hum Evol* 45:155–167.
6. Beaumont P (1978) Border Cave, PhD Thesis, University of Cape Town, South Africa.
7. Grün R, Beaumont P (2001) Border Cave revisited: a revised ESR chronology. *J Hum Evol* 40(6): 467–482.
8. Villa P, et al. (this issue) New directions in the evolution of technology: The beginning of the Later Stone Age in South Africa. *Proc Natl Acad Sci USA*
9. Millard A (2006) Bayesian analysis of ESR dates, with application to Border Cave. *Quat Geochronology* 1(2):159-166.
10. Miller G, Beaumont P (1989) Dating in the Middle Stone Age at Border Cave, South Africa, by the epimerization of isoleucine in ostrich eggshell. *Geol Soc Am* 21:A235.
11. Miller G, et al. (1999) Earliest modern humans in southern Africa dated by isoleucine epimerization in ostrich eggshell. *Quat Sci Rev* 18(13):1537–1548
12. Beaumont P (1980) On the age of the Border Cave hominids 1-5. *Palaeont Afr* 23:21–33.
13. Bird M, et al. (2003) Radiocarbon dating from 40 to 60 ka BP at Border Cave, South Africa. *Quat Sci Rev* 22(8–9): 943–947.
14. Bronk Ramsey C (2009) Bayesian analysis of radiocarbon dates. *Radiocarbon* 51:337–360.
15. Miller R (1975) Systematic anatomy of the xylem and comments on the relationships of the Flacourtiaceae. *J Arnold Arboretum* 56:20–102.
16. Coates Palgrave K (2002) *Trees of Southern Africa* (Struik Publishers, Cape Town).

17. Mennega A (1987) Wood anatomy of the Euphorbiaceae, in particular of the subfamily Phyllanthoideae. *Botanical J Linnean Soc* 94:111–126.
18. Tabuti J (2007) *Flueggea virosa* (Roxb. ex Willd.) Voigt. Plant Resources of Tropical Africa / Resources végétales de l'Afrique tropicale, eds Schmelzer G, Gurib-Fakim A, (Wageningen, Netherlands), http://database.prota.org/search.htm
19. Walton T (1990) Waxes, cutin and cuberin in *Methods in Plant Biochemistry, Lipids, Membranes and Aspects of Photobiology* vol 4, eds Harwood J, Bowyer J (Academic Press, London), pp 105–158.
20. Lucejko JJ, Lluveras-Tenorio A, Modugno F, Ribechini E, Colombini MP (2012) An analytical approach based on X-ray diffraction, Fourier Transform Infrared spectroscopy and gas chromatography-mass spectrometry to characterize Egyptian embalming materials. *Microchem J* 103:110-118.
21. Lluveras A, Bonaduce I, Andreotti A, Colombini M (2010) GC/MS analytical procedure for the characterization of glycerolipids, natural waxes, terpenoid resins, proteinaceous and polysaccharide materials in the same paint microsample avoiding interferences from inorganic media. *Anal Chem* 82:376–386.
22. Ribechini E, Modugno F, Colombini M, Evershed R (2008) Gas chromatographic and mass spectrometric investigations of organic residues from Roman glass unguentaria. *J Chromatogr A* 1183:158–169.
23. Bonaduce I, Colombini M (2004) Characterisation of beeswax in works of art by gas chromatography-mass spectrometry and pyrolysis-gas chromatography-mass spectrometry procedures. *J Chromatogr A* 1028:297–306.
24. Budzikiewicz H, Wilson J, Djerassi C (1963) Mass spectrometry in the structural stereochemical problems XXXII. Pentacyclic Triterpenes. *J Am Chem Soc* 85:3688-3699.
25. Seigler DS (1994) Phytochemistry and systematics of the *Euphorbiaceae*. *Ann Missouri Bot Garden* 81:380-401.
26. Kandel A, Conard N (2005) Production sequences of ostrich eggshell beads and settlement dynamics in the Geelbek Dunes of the Western Cape, South Africa. *J Archaeol Sci* 32:1711–1721.
27. Jacobson L (1987) The size variability of ostrich eggshell beads from central Namibia and its relevance as a stylistic and temporal marker. *S Afr Archaeol Bull* 42:55–58.
28. Orton J (2008) Later Stone Age ostrich eggshell bead manufacture in the Northern Cape, South Africa. *J Archaeol Sci* 35:1765–1775.
29. Barham L (1989) A preliminary report on the Later Stone Age artefacts from Siphiso Shelter in Swaziland. *S Afr Archaeol Bull* 44(149):33–43.
30. Shipman P, Rose J (1988) in *Scanning Electron Microscopy in Archaeology*, ed Olsen S (BAR Int Ser 452, Oxford) pp 303–335.
32. Backwell L, d'Errico F (2004) The first use of bone tools: a reappraisal of the evidence from Olduvai Gorge, Tanzania. *Palaeont Afr* 40:95–158.
33. Semenov S (1964) *Prehistoric Technology: An Experimental Study of the Oldest Tools and*

Artifacts from Traces of Manufacture and Wear (Harper Row Publishers, Great Britain).
34. d'Errico F, Giacobini G, Puech P-F (1984) An experimental study on the technology of bone-implement manufacturing. *MASCA J* 3(3):71–74.
35. d'Errico F (1993) La vie sociale de l'art mobilier paléolithique. Manipulation, transport, suspension des objets en os, bois de cervidés, ivoire. *Oxford J Archaeol* 12(2):145–174.
36. d'Errico F (1998) in *Cognition and Material Culture: the Archaeology of Symbolic Storage*, eds. Renfrew C, Scarre C (McDonald Institute Monographs, Cambridge:), pp 19–50.
37. Griffitts J (1993) *Experimental Replication and Analysis of Use-wear on Bone Tools*. MA Thesis. University of Colorado.
38. Choyke A, Bartosiewicz L (2001) *Crafting Bone: Skeletal Technologies Through Time and Space*, (BAR Int Ser 937, Oxford).
39. Backwell L, d'Errico F (2005) in *From Tools to Symbols. From Early Hominids to Modern Humans*, eds d'Errico F, Backwell L (Witwatersrand University Press, Johannesburg), pp 238–275.
40. Legrand A, Sidéra I (2007) in *Bones as Tools: Current Methods and Interpretations in Worked Bone Studies*, eds Gates St-Pierre C, Walker R (Oxbow, Oxford), pp 291–304.
41. Lesnik J (2011) Bone tool texture analysis and the role of termites in the diet of South African hominids. *Palaeoanthropology* 28:268–281.
42. Buc N (2011) Experimental series and use-wear in bone tools. *J Archaeol Sci* 38(3):546-557.
43. LeMoine G (1991) *Experimental Analysis of the Manufacture and Use of Bone and Antler Tools among the Mackenzie Inuit*. Ph.D. Thesis, University of Calgary, Alberta.
44. d'Errico F, Backwell L (2003) Possible evidence of bone tool shaping from the early hominid site of Swartkrans, South Africa. *J Archaeol Sci* 30:1559–1576.
45. d'Errico F, Henshilwood C (2007) Additional evidence for bone technology in the southern African Middle Stone Age. *J Hum Evol* 52:142–163.
46. Backwell L, d'Errico F, Wadley L (2008) Middle Stone Age bone tools from the Howiesons Poort layers, Sibudu Cave, South Africa. *J Archaeol Sci* 35:1566–1580.
47. d'Errico F**,** Moreno-Mazel R, Rifkin R (2011) Technological, elemental and colorimetric analysis of an engraved ochre fragment from the Middle Stone Age levels of Klasies River Cave I, South Africa. *J Archaeol Sci.* 39(4): 942–952.
48. Wanless A (2010) The Fourie collection of Khoisan ethnographica: forming an archive. *Social Dynamics* 36(1):24–37.
49. Goodwin A (1945) Some historical Bushman arrows. *South Afr J Sci* 61:429–443.
50. Deacon J (1992) *Arrows as Agents of Belief Amongst the /Xam Bushmen* (South African Museum, Cape Town).
51. d'Errico F**,** Henshilwood C, Vanhaeren M, van Niekerk K (2005) *Nassarius kraussianus* shell beads from Blombos Cave: Evidence for symbolic behaviour in the Middle Stone Age. *J Hum Evol* 48:3–24.
52. Crabtree D, Davis E (1968) Manufacture of wooden implements with tools of flaked stone. *Science* 159(3813):426-428.

53. Custance A (1968) Stone tools and woodworking. *Science* 160(3823):100–101.
54. Oakley K, Andrews P, Keeley L, Clark J (1977). A reappraisal of the Clacton spearpoint. *Proc Prehistoric Soc* 43:13–30.
55. Clark J (2001) *Kalambo Falls Prehistoric Site* III, *the Earlier Cultures: Middle and Earlier Stone Age* (Cambridge, Cambridge University Press).
56. Bamford M, Henderson Z (2003) A reassessment of the wooden fragment from Florisbad, South Africa. *J Archaeol Sci* 30: 637–650.
57. Bamford, M (2005) in *From Tools to Symbols. From Early Hominids to Modern Humans*, eds d'Errico F, Backwell L (Witwatersrand University Press), pp 103–120.
58. Thieme H (1997) Lower Palaeolithic hunting spears from Germany. *Nature* 385:807–810.
59. Nadel D, Grinberg U, Boaretto E, Werker E (2006) Wooden objects from Ohalo II (23,000 cal BP), Jordan Valley, Israel. *J Hum Evol* 50:644–662.
60. Binneman J (1994) Note on a digging stick from Augussie Shelter. *Southern African Field Archaeology* 3:112–113.
61. Opperman H (1996) in *Aspects of African Archaeology,* eds Pwiti G, Soper R (University of Zimbabwe, Harare), pp 335–342.
62. Colombini MP, Lucejko JJ, Modugno F, Orlandi M, Tolppa E-L, Zoia L (2009) A multi-analytical study of degradation of lignin in archaeological waterlogged wood. *Talanta* 80:61-70.
63. Fabbri D, Chiavari G (2001) Analytical pyrolysis of carbohydrates in the presence of hexamethyldisilazane. *Anal Chim Acta* 449:271-280.
64. Moldoveanu S (1998) in *Analytical Pyrolysis of Natural Organic Polymers,* eds Coleman D, Price B (Elsevier Science, Amstersdam), pp 217–316.
65. InsideWood (2004) http://insidewood.lib.ncsu.edu/search. Accessed 4 January 2010; February 2012.
66. Kromhout C (1975) n Sleutel vir die mikroskopiese uitkenning van die vernaamste inheemse houtsoorte van Suid-Afrika. *S Afr Dep Forestry Bull* 50:1–124.
67. Neumann K, Schoch W, Détienne P, Schweingruber F (2001) *Woods of the Sahara and the Sahel* (Paul Haupt, Bern).
68. Stuiver M, Polach H (1977) Discussion; reporting of C-14 data. *Radiocarbon* 19(3):355–365.
69. Vogel J, Fuls A, Visser E (2001) Suitability of ostrich eggshell for radiocarbon dating. *Radiocarbon* 43:1330–1337.
70. Freundlich J, Schwabedissen H (1989) Radiocarbon dating of ostrich eggshells. *Radiocarbon* 31(3):1030-1034.
71. Brock F, Higham T, Ditchfield P, Bronk Ramsey C (2010) Current pretreatment methods for AMS radiocarbon dating at the Oxford Radiocarbon Accelerator Unit (ORAU). *Radiocarbon* 52(1): 103–112.
72. Bronk Ramsey C, Higham T, Leach P (2004) Towards high-precision AMS: progress and limitations. *Radiocarbon* 46(1):17–24.
73. Bronk Ramsey, C., Higham T, Owen D, Pike A, Hedges R (2002) Radiocarbon dates from the Oxford AMS system: Archaeometry datelist 31. *Archaeometry* 44(3):1–149.

74. Reimer P, et al. (2009) Intcal09 and Marine09 radiocarbon age calibration curves, 0–50,000 years cal BP. *Radiocarbon* 51(4):1111–1150.
75. Bronk Ramsey, C (2009) Dealing with outliers and offsets in radiocarbon dating. *Radiocarbon* 51(3):1023–1045.
76. Reimer, P.J, et al. (2009) Intcal09 and Marine09 radiocarbon age calibration curves, 0–50,000 years cal BP. *Radiocarbon* 51(4):1111–1150.